THE EFFECTS OF HYDRATING AGENTS ON THE HYDRATION OF INDUSTRIAL MAGNESIUM OXIDE

by

KGABO PHILLEMON MATABOLA

Submitted in fulfilment of the requirements for
the degree of

MASTER OF SCIENCE

in the subject

CHEMISTRY

at the

UNIVERSITY OF SOUTH AFRICA

SUPERVISOR: DR E M VAN DER MERWE

JOINT SUPERVISOR: PROF C A STRYDOM

NOVEMBER 2006

ABSTRACT

Magnesium hydroxide, a stable flame retardant, can be obtained by mining or by the hydration of magnesium oxide. In this study, the effect of different hydrating agents on the pH of the hydrating solution, rate of hydration of MgO to $Mg(OH)_2$ and product surface area were studied as a function of the temperature of hydration.

Ammonium chloride, magnesium acetate, magnesium nitrate, nitric acid, acetic acid, water, magnesium chloride, sodium acetate and hydrochloric acid were used as hydrating agents. The hydration experiments were carried out in a water bath between 30 - 80 ^{o}C for 30 minutes. Dried MgO samples were introduced to the hydrating solution and the slurry was stirred at a constant speed. At the end of each experiment, the slurry was vacuum filtered, washed with water, dried at 200 ^{o}C and hand ground. The products were then characterized by TGA, XRF, XRD and BET surface area analyses.

There was not a significant difference in the hydration behaviour of the hydrating agents up to 50 ^{o}C, where less than 10 % of magnesium hydroxide was formed. When compared to the hydration in water, all the hydrating agents with the exception of sodium acetate showed a significant increase in the degree of hydration. Sodium acetate formed the lowest amount of magnesium hydroxide, ranging between 1.2 and 12.2 % magnesium hydroxide. Hydrations performed in hydrochloric acid and magnesium nitrate formed the largest percentage (11.8 %) of magnesium hydroxide at 60 ^{o}C. Magnesium acetate, magnesium nitrate, magnesium chloride and hydrochloric acid seemed to be the most effective hydrating agents at 70 ^{o}C with the percentage magnesium hydroxide being formed ranging between 20.0 and 23.9 %. The amount of hydroxide formed doubled at 80 ^{o}C, with the largest percentage (56.7 %) formed from the hydration in magnesium acetate.

The hydration reaction seemed to be dependent upon the presence of Mg^{2+} and acetate ions. It seemed that magnesium oxide hydration is a dissolution-precipitation process controlled by the dissolution of magnesium oxide. The results have also indicated that the pH and temperature of the hydrating solution strongly influence the degree of hydration.

ACKNOWLEDGEMENTS

I would like to express my sincere appreciation to the following people for their kind help, support and encouragement throughout this study:

- My supervisor, Dr E M Van der Merwe, for her valuable guidance, advice, support and for getting me interested in the study
- My co-supervisor, Prof C A Strydom (UP), for her helpful comments
- Chamotte Holdings (Pty) LTd, for providing the MgO sample
- I am grateful to Mrs Maggie Loubser and Dr Sabine Verryn of University of Pretoria (X-ray lab) for the provision of XRF and XRD data respectively
- I am of course, indebted to Unisa and NRF, for providing funding for this study.
- The support of chemistry chairperson, Prof M J Mphahlele, and the rest of the Chemistry staff is also acknowledged
- Finally, I am very grateful to both my parents for supporting me while I was working on this study

LIST OF ABBREVIATIONS

LOI	:	Loss On Ignition
N	:	Normality
M	:	Molarity
rpm	:	revolutions per minute
BET	:	Brunauer, Emmet and Teller
kV	:	Kilo volt
keV	:	Kiloelectron volt
TG	:	Thermogravimetry
XRF	:	X-ray fluorescence
XRFS	:	X-ray fluorescence spectrometry
XRD	:	X-ray diffraction
T_f	:	Furnace temperature
T_s	:	Sample temperature
g/l	:	gram per liter
μg/g	:	microgram per gram

MINERAL NAMES

Periclase	:	MgO
Magnesite	:	$MgCO_3$
Brucite	:	$Mg(OH)_2$
Dolime	:	$CaO.MgO$
Dolomite	:	$CaMg(CO_3)_2$
Lime	:	CaO
Carnallite	:	$KMgCl_3.6H_2O$
Gypsum	:	$CaSO_4.2H_2O$
Quartz	:	SiO_2
Serpentinites	:	$Mg_3Si_2O_5(OH)_4$
Calcite	:	$CaCO_3$
Woolastonite	:	$CaSiO_3$
Aragonite	:	$CaCO_3$

TABLE OF CONTENTS

LIST OF FIGURES

LIST OF TABLES

CHAPTER 1

INTRODUCTION

1.1 Problem statement

Magnesium hydroxide, a very popular, environmentally friendly and thermally stable flame-retardant filler in composite materials, can be used to neutralize acidic waste streams, as fertilizer, and/or as the most important precursor in the manufacturing of magnesium oxide. It can be prepared by several methods, such as hydration of magnesium oxide, electrolysis of aqueous solutions of magnesium salt, sol-gel techniques, and precipitation (Hsu, et al., 2005) or it can be mined as the mineral called brucite. Natural magnesium hydroxide (brucite) deposits are rare but do occur in nature. The disadvantage associated with the mined mineral is the large number of additional minerals such as calcite, woolastonite, aragonite, dolomite, etc that occur with it in most instances. This results in a need for various separation procedures to isolate the required product.

Magnesium hydroxide obtained from the hydration of magnesium oxide has the advantage of being purer due to controlled experimental conditions. The quality and amount of the hydroxide formd depends on the reactivity of magnesium oxide used as a precursor**.** The products obtained can be characterized with various techniques to determine the success rate of the method.

The present study reveals the effect of different hydrating agents on the hydration of industrially obtained magnesium oxide over the temperature range of 30 ^{o}C to 80 ^{o}C. The effect of temperature and pH on the degree of hydration and product surface area will be studied.

1.2 Uses of magnesium hydroxide

The largest use of magnesium hydroxide is for environmental applications, which include industrial water treatment, heavy-metals removal, and flue-gas desulfurization. For water treatment, magnesium hydroxide is supplied as a suspension containing about 58 % solids, and is used primarily to raise the pH of acidic solutions. Magnesium hydroxide competes with other acid-neutralizing compounds in the market, of which the most common are lime and caustic soda. Magnesium hydroxide has advantages and disadvantages when compared to the other materials with similar uses. One of the advantages is that it is a pH buffer, and wastewater treated with it will not exceed a pH of 9.5 even if excess magnesium hydroxide is added. In contrast, excess addition of lime can raise the pH to 12, and excess caustic soda addition can raise the pH to 14. In these cases, back additions of acid are necessary to lower the pH (Kirk-Othmer, 2005).

Magnesium hydroxide is better than lime or caustic soda at removing metals such as lead and trivalent chromium. Metal hydroxides that are precipitated with magnesium hydroxide rather than caustic soda or lime tend to form larger crystals, resulting in lower sludge volumes and hence, lower disposal costs. The solids formed through precipitation by magnesium hydroxide have a cakelike consistency, rather than that of a gel as do the solids formed by caustic soda precipitation, and therefore the cake is easier to handle (Alvin, et al., 1994).

In flue-gas desulphurisation, magnesium hydroxide is employed in place of lime and gypsum, particularly in power generation and waste incineration plants. Scrubbing with lime produces gypsum, which needs to be land filled in most cases whilst with sodium hydroxide is prohibitively expensive. Incineration plants generate acidic gases and molten salt-based slag. These gases corrode the incinerator walls and metals in their vicinity. Also salt-based slag often causes crustification on the incinerator walls and plugs the vents. This in some cases leads to plant shut down. Adding magnesium hydroxide, in slurry or powder form, to the waste neutralizes the acidic gases and also minimises slag formation and build-up on incinerator walls by increasing the melting point temperature of the molten slag (Aral, et al., 2004).

The second largest use for magnesium hydroxide is as a precursor for other magnesium chemicals. About 5 % of magnesium hydroxide is used in pharmaceuticals. The pharmaceutical grades of magnesium hydroxide include a 100 % magnesium hydroxide powder used in antacid tablets and a 30 % suspension used in liquid antacids such as milk of magnesia (Aral, et al., 2004).

Like magnesium carbonate, magnesium hydroxide can replace alumina trihydrate in some flame retardants. Both alumina trihydrate and magnesium hydroxide function as flame retardants by releasing water vapor in an endothermic reaction that diverts the heat away from the flame, thereby reducing the formation of combustible gases. Alumina or magnesia remaining after the water is released is believed to have a high surface area available for absorbing smoke. Although the properties of alumina trihydrate and magnesium hydroxide are similar, magnesium hydroxide has a higher temperature stability. Magnesium hydroxide begins to decompose at about 330 ^{o}C, compared to about 200 ^{o}C for alumina trihydrate. This higher temperature stability makes magnesium hydroxide more attractive for flame retardant applications (Kirk-Othmer, 2005).

1.3 Properties of $Mg(OH)_2$

The physical properties of magnesium hydroxide are listed in Table 1.1. The crystalline form of magnesium hydroxide is uniaxial hexagonal platelets. Magnesium hydroxide begins to decompose thermally at about 330 ^{o}C and the last traces of water are driven off at higher temperatures to yield magnesia. Upon exposure to the atmosphere, magnesium hydroxide absorbs moisture and carbon dioxide (Kirk-Othmer, 2005).

Table 1.1. Physical Properties of Magnesium Hydroxide (Kirk-Othmer, 2005)

Property	Value
mol wt	58.32
crystal system	hexagonal
space group	P3 ml
lattice constants, nm	
a	0.3147
c	0.4769
Z[a]	1
density, g/cm^3	
$Mg(OH)_2$	2.36
brucite	2.38-3.40
index of refraction	1.559, 1.580
colour	colourless to white
hardness, Mohs'	2.5
decomposition temperature	
brucite	268 ^oC [b]
$Mg(OH)_2$	350 ^oC [b]
solubility,[c] mg/l	
25 ^oC	11.7
100 ^oC	4.08
solubility product, K_{sp}, at 25^oC	5.61 x 10^{-12}
heat of formation, ΔH_{298}, kJ/mol	-924.54
free energy of formation, ΔG_{298} kJ/mol	-833.58
C_p,298, J/(mol.K)	77.03

[a]Number of formula per unit cell.

[b]Begins to lose H_2O.

[c]There is only fair agreement between data of various authors.

1.4 Hydration of MgO

1.4.1 Proposed mechanisms

Rocha et al. (2004) obtained magnesium hydroxide by hydrating magnesia in water as indicated by:

$$MgO\ (s) + H_2O\ (l) \rightarrow Mg(OH)_2\ (s).$$

Although it seems to be a simple operation, the kinetics of magnesia hydration must be carefully controlled so as to obtain a hydroxide with the desired properties. Fillipou et al. (2004) indicated that very rapid hydration of magnesia will result in the formation of relatively large hydroxide aggregates consisting of submicroscopic crystallites with high surface area- particle morphology that is unacceptable for certain applications. Furthermore, the quality of the hydroxide depends on the magnesium oxide used as precursor.

Rocha et al. (2004) proposed that the reaction mechanism of the above reaction comprises steps of magnesia dissolution followed by magnesium hydroxide precipitation. Fruhwirth et al. (1985) reported an epitaxial growth of the hydroxide at the magnesium oxide surface in water vapour. A quite similar mechanism for magnesia hydration has been proposed assuming water molecules adsorb chemically at the oxide surface, creating a surface layer of magnesium hydroxide at the surface of the solid. The magnesium hydroxide layer imposes an additional resistance that limits the hydration reaction process (Fruhwirth, et al., 1985).

The chemical adsorption of water on the metallic oxide surface is given by (Rocha et al., 2004):

$$MgO\ (s) + H_2O\ (l) \rightarrow Mg(OH)_2\ (s)$$
$$\rightarrow MgOH^+\ (surface) + OH^-\ (aq)$$

thus indicating the surface of magnesium oxide is hydroxylated in the presence of water, i.e. it contains OH^- in equilibrium with $MgOH^+$ sites at the surface of the solid. The mechanism of magnesia hydration involves the formation of $MgOH^+$ ions adsorbed at the surface of the solid particles as shown by the above reaction. The authors suggest that $MgOH^+$ sites seem to predominate on the MgO surface at pH

values below 12.5 ± 0.5. It was also indicated that $MgOH^+$ ions do not predominate in solution below pH 11.5. Therefore, the Mg^{2+} and OH^- ions predominate at pH values ranging between 7 and 11.5, so that the following reaction may occur in the system:

$$MgOH^+ (surface) \rightarrow Mg^{2+} (aq) + OH^- (aq)$$

The hydroxide can be removed from the reagents' surface by dissolution. Rocha et al. (2004) indicated that the solubility of magnesium hydroxide reduces as the temperature of the system is raised. Fruhwirth et al. (1985) suggested that the OH^- ions' adsorption followed by the Mg^{2+} ions' desorption are critical steps in dissolving magnesium hydroxide in solution at pH values below 11.5.

Rocha et al (2004) suggested two distinct processes of hydration occurring depending on the temperature. At high temperatures, the hydration of magnesia seems to be initially governed by the oxide dissolution (chemical control), but as the reaction progresses, both surface and pores of magnesia particles are progressively covered by the magnesium hydroxide produced, changing the porosity of the solid. As a result, the diffusion of water is hindered inside the particles, thus reducing the overall reaction rate (diffusive control). At low temperatures the hydration is purely chemically controlled because conversion is relatively low. These authors suggested that the reaction is controlled by the oxide dissolution, and the mechanism consists of the following steps:

(1) Water adsorbs at the surface and diffuses inside porous MgO particles,
(2) Oxide dissolution occurs within particles, changing porosity with time, and
(3) Creation of supersaturation, nucleation and growth of magnesium hydroxide at the oxide surface.

Feitknecht and Braun (1967) synthesized magnesium hydroxide by the hydration of magnesium oxide in water vapour and the following reaction mechanism was proposed:

(1) Initially water vapor is physically adsorbed on the MgO and then chemisorbed to form an aqueous layer on the surface of the solid,
(2) This layer of water reacts with the MgO to form a surface layer of magnesium hydroxide,
(3) The magnesium hydroxide subsequently dissolves in the water layer, and finally

(4) As the water layer becomes saturated with $Mg(OH)_2$, precipitation takes place.

Literature indicated that two surface chemical reactions take place when MgO reacts with water and goes into solution as Mg^{2+} and OH^- (Smithson et al., 1969). These are the formation of $Mg(OH)_2$ and the removal of $Mg(OH)_2$ as Mg^{2+} and OH^- ions from the MgO surface from the MgO surface, of which the second is the rate controlling step (Feitknecht, et al., 1967, Smithson, et al., 1969).

Filippou et al (1999) studied the kinetics of magnesia hydration in the presence of acetate ions. In that particular study it was observed that the hydration of magnesia clinker (hard-burnt magnesia) in aqueous solutions of 0.1 $mol.dm^{-3}$ magnesium acetate over the temperature range of 70 – 100 ^oC proceeds in stages. In the initial stage, magnesium hydroxide forms and covers each magnesia particle, causing low hydration rates due to product-layer diffusion control. As the degree of hydration increases beyond 15 %, the magnesium hydroxide layer starts cracking and peeling off from the mother magnesia particle. This is the second process stage and is surface-reaction controlled. In the last process stage, all small magnesia particles are totally converted to magnesium hydroxide while the few relatively large magnesia particles continue to hydrate very slowly. The hydration of magnesia clinker in 0.1 $mol.dm^{-3}$ magnesium chloride solutions was found to proceed in a different way. It was observed that in the latter system, $Mg(OH)_2$ forms on magnesia particles but does not peel off, hence the degree of hydration remains less than about 80 % even after 40 h. It was also observed that the morphology of the end product was different; in the acetate system, the hydroxide produced had the form of hexagonal plates of uniform diameter, while elongated hexagonal prisms were obtained in the chloride system.

Filippou et al (1999) suggested the following hydration reaction mechanism in the presence of acetate ions:

(1) Magnesium acetate dissociation:

$$(CH_3COO)_2Mg\ (aq) \leftrightarrow 2\ CH_3COO^-\ (aq) + Mg^{2+}\ (aq)$$

(2) Magnesia dissolution:

$$MgO\ (s) + CH_3COO^-\ (aq) + H_2O\ (l) \leftrightarrow CH_3COOMg^+\ (aq) + 2OH^-\ (aq)$$

Or even by direct attack by acetic acid which is formed in the bulk of the solution:

$CH_3COO^-(aq) + H_2O(l) \rightarrow CH_3COOH(aq) + OH^-(aq)$

$MgO(s) + CH_3COOH(aq) \rightarrow CH_3COOMg^+(aq) + OH^-(aq)$

(3) Dissociation of magnesium complexes and magnesium hydroxide precipitation in the bulk of the solution due to supersaturation:

$CH_3COOMg^+(aq) \rightarrow CH_3COO^-(aq) + Mg^{2+}(aq)$

$Mg^{2+}(aq) + 2\,OH^-(aq) \rightarrow Mg(OH)_2(s)$

The above mechanism provides an explanation for the enhanced rate of magnesia hydration in the presence of acetate ions. It was observed that the rate of magnesia hydration in 0.75 $mol.dm^{-3}$ NaOH without any acetate ions is higher than that in pure water, but lower than in 0.022 $mol.dm^{-3}$ magnesium acetate. Moreover, Nakanishi et al (1987) observed that the rate of magnesia hydration is considerably lower in magnesium chloride solutions than in magnesium acetate.

Literature has indicated that the reaction mechanism comprises steps of magnesia dissolution with further magnesium hydroxide precipitation controlled by the dissolution of MgO (Rocha, et al, 2004, Fillipou, et al., 2004, Feitnecht, et al., 1967, Nakanishi et al., 1987). The physical properties of the solid reagent were found to strongly influence the hydration reaction (Birchal, et al., 2001).

Van der Merwe et al (2004) studied the extent to which different parameters (concentration of magnesium acetate, solution temperature and solid to liquid ratio of MgO) influence the hydration rate of a medium reactive magnesium oxide. Various other ions, e.g. Mg^{2+} and CH_3COO^-, in solutions may influence the rate of formation of the hydroxide (Botha, et al., 2001). Birchal et al (2000), Strydom et al (2005) and Maryska et al (1997) have studied the effects of calcining temperature and time on the hydration of industrially obtained magnesium oxide. They all found that the degree of hydration is influenced considerably by calcining temperature and time.

Raschman et al (2004) studied the kinetics of the reaction between dead-burnt magnesia and hydrochloric acid. The effect of temperature, activity of H^+ ions, particle size and composition of the solid on the dissolution of magnesium oxide was

investigated. Chemical dissolution of burnt magnesite in hydrochloric acid is a liquid-solid reaction in which no solid product is formed. The following overall hydration process was proposed which involves the following steps in series:

(1) Diffusion of H^+ ions through the liquid film at the liquid-solid interface to the surface of the solid particles,

(2) Surface chemical reaction according to the equation below:

$$MgO\ (s) + 2\ H^+(aq) \rightarrow Mg^{2+}(aq) + H_2O\ (l)$$

(3) Diffusion of liquid products from the interface through the film to the bulk liquid.

Fruhwirth et al (1985) suggested that the precipitation rate is limited by the dissolution rate of MgO and that magnesium hydroxide precipitation sets in immediately after the supersaturation period. The authors indicated three models for the rate of hydration when a new phase is formed:

(1) Control by the dissolution of MgO,

(2) Control by transport of ions from MgO to $Mg(OH)_2$,

(3) Control by $Mg(OH)_2$ crystal growth

1.4.2 Factors that influence the degree of hydration

The hydration rate of magnesium oxide depends on the temperature of hydration as well as the grade of magnesium oxide. However, a decisive influence on the hydration rate is exhibited by the degree of crystallization and sintering of magnesium oxide, whose measure is its specific surface area (Maryska, et al., 1997). Smithson et al (1969) reported that the hydration rate is directly proportional to the surface area of the magnesium oxide particles.

An increase in the calcining temperature results in a decrease in the degree of hydration (de Mille Campbell, 1918). The most reactive magnesium oxide sample with the lowest activity value and highest specific surface area shows the highest degree of hydration and the less reactive magnesium oxide sample with the highest activity value and lowest specific surface area shows the lowest degree of hydration (Birchal, et al., 2001). The activity value, expressed as the time needed to completely neutralize the acid, is taken as a measure of the solid reactivity. It was also found that

the rate of hydration increases with a decrease in particle size and therefore an increase in surface area (Raschman et al., 2004). Van der Merwe et al (2004) observed that hydration time plays a role in enhancing the degree of hydration. The type and amount of magnesium oxide used during hydration have a huge effect on the rate of hydration. A decrease in the solid to liquid ratio of magnesium oxide used during hydration may result in lower amounts of magnesium hydroxide being formed. The degree of hydration can be doubled when an optimum solid to liquid ratio of magnesium oxide to hydrating agent is used.

The hydration rate can also be increased by increasing the hydrating agents' concentration (Van der Merwe, et al., 2004), by using different types of hydrating agents (Van der Merwe, et al., 2006) and by changing the pH or by adding salts (Jost, et al., 1997).

1.4.3 Hydration methods of MgO

The hydration of magnesium oxide to magnesium hydroxide can be achieved by numerous methods. Some of these will be discussed below.

A mixture containing burnt natural magnesite and water is pressure-hydrated in an autoclave at elevated pressures to produce precursory magnesium hydroxide slurry. The slurry is then stabilized by subjecting it to chemical and mechanical treatment. The chemical treatment is accomplished by addition of chloride ions and cationic polymers. The chloride ions are added to the hydrator prior to hydration to cause a larger particle size distribution exiting the hydrator, but the larger particles can be deagglomerated. Cationic polymers which are unstable at the hydration temperature are added after hydration to adjust the viscosity to within an acceptable range. Mechanical treatment is performed to deagglomerate the product and disperse any desired additives. The magnesium hydroxide slurry produced by pressure hydration has many advantages above atmospheric hydration, some of which are mentioned below (Witkowski et al., 1996):

(1) Hydration time is significantly reduced,
(2) The particle size distribution of the product is smaller than that of the atmospheric hydrate,

(3) Maintenance costs are reduced since the pressure hydration products are easier to deagglomerate and stabilize, and
(4) Pumping and agitation costs are low.

Another method comprises a wet-pulverizing means for comminuting magnesia in the wet state and a reaction vessel for hydrating the resultant pulverized magnesia in the presence of a heated alkaline aqueous medium at a temperature of not less than 70 ^{o}C. The product obtained is of uniform quality, high activity and low viscosity at a high concentration (Akihiko, 1994).

Hydrogel magnesium hydroxide with a high reactivity can be prepared by treating finely crushed magnesium oxide with water at temperatures higher than 85 ^{o}C and a reaction time between 20 min and 5 hours. Sodium hydroxide is added to the MgO and water as a hydration accelerator (Shinoda, 1989).

Magnesium hydroxide can also be manufactured by hydrating magnesium oxide in an aqueous medium containing alkali metal ions, alkaline earth metal ions, and/or NH_4^+ and OH^-, NO_3^-, CO_3^{2-}, Cl^- and /or SO_4^{2-} ions. The calcined magnesium oxide was crushed, mixed in water with sodium hydroxide, filtered and dried to give magnesium hydroxide (Nakamura, et al., 1989).

1.5 Natural sources of magnesium oxide

Periclase (MgO) is an extremely rare mineral and does not occur in commercial quantities. About 70 % of the world's magnesia production comes from magnesium – rich minerals.

1.5.1 Brucite ($Mg(OH)_2$)

Magnesium oxide is produced by calcination of magnesium hydroxide. Depending on the calcination temperature, several forms of magnesia may be produced.

1.5.2 Magnesite ($MgCO_3$)

The theoretical MgO content of magnesite, $MgCO_3$, is 47 % so that magnesite represents a concentrated source of magnesia. The magnesites occur in two physical forms, crystalline and cryptocrystalline. The crystalline form typically has a crystallite size in the range 50-200 μm. Impurity levels can be relatively high, giving the magnesite a color ranging from off-white to dark brown. Most crystalline magnesites are intimately associated with dolomite, which may occur as discrete bands or lenses. Cryptocrystalline are very fine-grained (≤20μm) magnesites which are usually associated with serpentinites, from which they are believed to have been formed. The deposits are usually quite pure and normally off-white in color (Canterford, 1985).

1.5.3 Dolomite ($[CaMg(CO_3)_2]$)

Many crystalline magnesite deposits contain appreciable amounts of dolomite ($[CaMg(CO_3)_2]$). In the seawater process, magnesium hydroxide is precipitated by addition of calcium oxide (lime), prepared by calcination of limestone or dolomite. Calcined dolomite (often termed dolime), has the advantage over calcined limestone in that it also contributes substantially to the amount of magnesia produced (Canterford, 1985).

1.5.4 Seawater, brines and bitterns

In open oceanic areas, the composition of seawater is remarkably constant, with a total dissolved solids content of about 35 g/L. The magnesium content is about 1.3 g/L. Brines and bitterns are more concentrated salt solutions having concentrations typically 3 and 40 times that of seawater, respectively. There are many natural brines ($CaCl_2$), the best known being the Dead Sea containing about 41 g/L magnesium. Other important sources of magnesia-rich brines are salt beds. The most important magnesium mineral in such deposits is carnallite, $KMgCl_3.\ 6H_2O$ (Canterford, 1985).

1.6 Grades of magnesium oxide

Depending on the calcination temperature, several forms of magnesia may be produced:

1.6.1 Caustic-calcined or soft burnt magnesia is prepared by calcining magnesium carbonate above 600 ^{o}C and up to 1000 ^{o}C (Aral et al., 2004). It is characterized by a small crystallite size, relatively large surface area (1.0-200 m^2/g), and moderate to high chemical reactivity (Kirk-Othmer, 2005). Due to the wide reactivity range that can be achieved for the product, industrial applications for caustic calcined magnesia are quite diverse. This grade of magnesium oxide readily dissolves in dilute acids and easily converts to magnesium hydroxide upon exposure to moisture (Aral et al., 2004). The reactivity of light-burnt magnesia is often quantified by its specific surface area, iodine number, rate of reaction in acetic acid, and rate of reaction with citric acid (Kirk-Othmer, 2005).

1.6.2 Hard-burnt magnesia is produced by the calcination of magnesia at temperatures in the range 1100 ^{o}C-1650 ^{o}C. It is characterised by a moderate crystallite size and moderately low chemical reactivity (due to a surface area of 0.1 to 1.0 m^2/g). Hard burnt magnesia is readily soluble in concentrated acids (Aral, et al., 2004).

1.6.3 Dead-burnt magnesia is prepared by calcining magnesia above 1450 ^{o}C and up to 2200 ^{o}C (Aral, et al., 2004). It is characterized by a large crytallite size and very low chemical reactivity (Kirk-Othmer, 2005). The magnesium oxide is referred to as 'dead-burnt' since, with a surface area of less than 0.1 m^2/g, most if not all, of the reactivity has been eliminated. It reacts very slowly with strong acids, and does not readily hydrate or react with carbon dioxide unless finely pulverized (Aral, et al., 2004).

1.6.4 Fused magnesia is produced from caustic-calcined magnesia or soft burnt, dead burnt magnesia or raw magnesite by calcining at temperatures between 2800 ^{o}C and 3000 ^{o}C (Aral, et al., 2004). Fused magnesia has an extremely large crystal size and may have single crystals weighing 200 g or more (Kirk-Othmer, 2005).

1.7 Properties and uses of magnesium oxide

Magnesium oxide, MgO, also known as magnesia, occurs in nature only infrequently as the mineral periclase, most commonly as groups of crystals in marble. The physical properties of periclase are given in Table 1.2 (Kirk-Othmer, 2005).

One of the important characteristics of magnesium oxide is that it has a melting point of above 2800^{o}C, so it is stable at high temperatures. Oxides that are even better than magnesium oxide in this respect include thorium oxide and uranium oxide. However, both thorium oxide and uranium oxide are radioactive substances. Magnesium oxide is therefore rated as the most heat-resistant oxide for practical applications. It also has good heat conductivity. Beryllium oxide is the only oxide that is more heat-conductive, but it is also toxic. In practical terms, therefore, magnesium oxide is the most heat-conductive oxide readily available. With excellent electric resistance, magnesium oxide is a highly insulative material that is characteristically less prone to degradation when heated. In addition, magnesium oxide is a safe material for the human body. All things considered, magnesium oxide is a very versatile oxide material (URL-1).

The end uses of magnesia are therefore highly dependent on the calcination temperature achieved. Dead-burnt magnesia is used in the form of refractory bricks in cement kilns, furnaces, ladles, glass-tanks checkers, and secondary refiring vessels in the metals refining industry and as components of refractory ‘gunning’ (sprayed) mixtures. Refractory grade magnesium oxide has a very high resistance to thermal ‘shock’ and is used extensively in steel production to serve as both protective and replaceable linings for equipment used to handle molten steel. Fused magnesia has excellent strength, abrasion resistance, and chemical stability translating to superior refractory performance and erosion resistance (Aral, et al., 2004).

Table 1.2. Physical Properties of Periclase (Kirk-Othmer, 2005)

Property	Value
mol wt	40.304
crystal form	fcc
lattice constant, nm	0.42
density, g/cm^3	3.581
index of refraction	1.732
hardness, Mohs'	5.6-6.0
melting point, ^{o}C	2827± 30
thermal conductivity at 100^{o}C, J/(s.cm. ^{o}C)	0.360
electrical resistivity, Ω.cm	
at 27 ^{o}C	1.3 x10^{15}
727 ^{o}C	2 x10^7
1727 ^{o}C	4 x 10^2
specific heat,kJ/(kg. K)	
at 27 ^{o}C	0.92885
227 ^{o}C	1.1255
727 ^{o}C	1.2719
1727 ^{o}C	1.3389
2727 ^{o}C	1.3598
heat of fusion at 2642^{o}C kJ/mol	77.4
heat of formation, ΔH_{298}, kJ/mol	-601.7
free energy of formation, ΔG_{298}, kJ/mol	-569.44
aqueous solubility, g/100 mL	
at 20 ^{o}C	0.00062
30 ^{o}C	0.0086

The industrial applications of magnesium oxide (or magnesium hydroxide) include waste water and sewage treatment (e.g. silica and heavy metals precipitation), scrubbing sulfur dioxide and sulfur trioxide from industrial flue gases and as a neutralizing agent for some industrial wastewater streams. Magnesium oxide is also used in several metallurgical applications, for example, caustic-calcined or light burnt magnesia is used in lateritic nickel production to precipitate a crude nickel cobalt hydroxide from sulphuric acid leach liquor. Magnesia is used in production of direct reduced iron and steel which is the largest user of refractory grade magnesia (Aral, et al., 2004).

Magnesia is also used in agricultural applications for animal feeds and as a fertilizer. Magnesium serves as a structural part of the chlorophyll molecule, a compound necessary for plant photosynthesis. Without sufficient magnesium, either from the soil or from fertilizer application, plants can die. Corn, potatoes, cotton, citrus, tobacco, and sugar beets are among the crops that are highly responsive to magnesium fertilization. Pasture fertilization with magnesium-containing fertilizers is also important in animal nutrition. Grazing ruminants, such as cattle and sheep, require magnesium in their diet to guard against hypomagnesia, also known as grass tetany, a potentially fatal disease. This disease most often occurs in cool weather when the animals are grazing on grass that has had a quick growth spurt. Two of the most popular methods of introducing magnesium in cattle diets are to incorporate the magnesium with molasses in a liquid lick, or adding caustic-calcined or light burned magnesia to purchased feed (Kirk-Othmer, 2005).

Magnesium oxides also find use in magnesium cements. Magnesium cements comprise two main groups, sorel cements and the much newer magnesium phosphate cements. Sorel cements are used particularly as so-called ‘magnesite’ flooring in industrial and institutional buildings. They are also consumed in making wallboards, fibreboards, refractory boards for fire doors, tiles and non-abrasive binders in grinding wheels and disks. Their use is restricted to indoor applications as the cement potentially is unstable in wet external conditions. Magnesium phosphate cements are used in rapid setting compositions and patching mortars for roadways, carparks and airport runways. Magnesium phosphate cements are unaffected by moisture and can be used in contact with steel reinforcing where the contained but strongly bound

phosphate passivates the steel to prevent corrosion (Aral, et al., 2004). Magnesia is also used as a stabilizer or vulcanizing agent in rubber. Fused and boron-free magnesia or periclases are used for insulation of heating elements in electric furnaces and appliances (Kirk-Othmer, 2005).

In manufacturing industries, caustic-calcined or light burnt magnesia is used in the production of rayon, fuel additives, lubricating oils and rubber. In the rubber industry caustic-calcined magnesia is used as a vulcanising agent in the curing of rubbers and elastomers. Magnesium oxide may be injected into oil-fired utility boilers to prevent scale build up. In oil well drilling muds and composition fluids, magnesia is used as a buffer for viscosity control, a corrosion inhibitor, and for cementing or closing off porous strata to prevent fluid loss and improve cutting efficiencies. Magnesia has applications as a low cost white pigment and functional filler for paints, varnish, plastics and rubber (Aral et al., 2004). Caustic–calcined or light burned magnesia is used to produce magnesium acetate, which is used for neutralization purposes in producing rayon fiber (Kirk-Othmer, 2005).

Magnesium oxide is an important raw material for many other magnesium chemicals and value-added products. In these applications caustic calcined magnesia is used as a magnesia source due to its higher reactivity (Aral, et al., 2004).

1.8 The aims of the study

The main objective of the study is to investigate the effect of different hydrating agents on the hydration of industrially obtained MgO, and also to study the effect of pH and temperature on the degree of hydration and the surface areas of the products.

The hydrating agents used were ammonium chloride, magnesium acetate, magnesium nitrate, nitric acid, acetic acid, water, magnesium chloride, sodium acetate and hydrochloric acid. The acidic hydrating agents were chosen because the MgO solubility is increased with an increase in H^+ concentration. The bases were chosen as hydrating agents to gain more insight into the dissolution and hydration steps on the alkaline side of the pH scale (Jost et al., 1997). Literature indicated that in strong basic regions, above pH 12, the degree of hydration greatly decreases because of the high OH^- concentration in the solution. The Mg containing compounds were chosen because literature indicated that a rapid and complete hydration requires a high content of Mg^{2+} ions in the aqueous solution, especially in acidic regions (Jost, et al., 1997).

CHAPTER 2

THEORETICAL BACKGROUND ON EXPERIMENTAL TECHNIQUES

2.1 Thermogravimetry

Thermogravimetry (TG) is a technique whereby a sample is continuously weighed as it is heated at a constant temperature for a specific time, at a constant heating rate, or a constant rate of mass loss. The resulting weight change against temperature curve obtained gives information concerning the thermal stability and composition of the original sample, intermediate compounds, and the residue (Wendlandt, 1964).

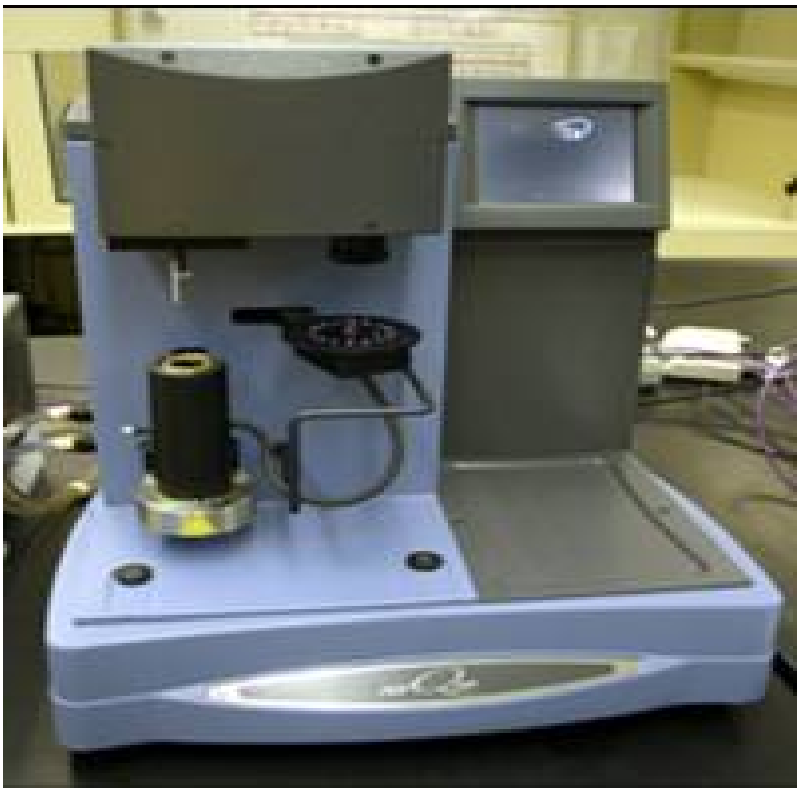

Figure 2.1. A picture of the TGA Q500, T A Instruments

Measurements of changes in sample mass with temperature are made using a thermobalance (Brown, 1988). The principal elements of a thermobalance are an electronic microbalance, a furnace, a temperature programmer, an atmospheric controller and a computer for simultaneously recording the output from these devices (Hatakeyama et al., 1998). The instrument used during this study was the TGA Q500 from TA Instruments. The instrument can measure in a temperature range of 20 ^{o}C up to 1000 ^{o}C. A simplified picture of the TGA Q500 from TA Instruments is given in Figure 2.1.

2.1.1 Factors affecting thermogravimetry:

The factors that influence the thermogram of a sample fall into two categories: (1) instrumental factors and (2) sample characteristics.

2.1.1.1 Instrumental factors

(a) Heating rate

A fast heating rate increases the temperature at which a reaction appears to start and at which the rate of weight-loss reaches a maximum, furthermore, it extends the range over which a weight-loss is observed. The resolution of overlapping reactions is generally decreased by very fast or very slow rates and a compromise rate should be chosen giving the narrowest weight-loss range but retaining detail in regions of rapid loss. A heating rate of 5 to 10 ^{o}C / min is usually satisfactory, but it will depend upon the sample and the apparatus (Daniels, 1973).

(b) Atmosphere

Fine control over the atmosphere in the vicinity of the sample is desirable since the use of different atmospheres is part of the technique of TG. This control usually involves the choice of a reactive or inert gas, its pressure and whether it is static or flowing. The main disadvantage of using a static atmosphere is the possibility of reaction products condensing on the cooler parts of the instrument. These may

corrode the balance mechanism or cause a weighing error if deposited on the pan support (Daniels, 1973). A flowing atmosphere has the advantages that it: (1) reduces condensation of reaction products on cooler parts of the weighing mechanism, (2) flushes out corrosive products, (3) reduces secondary reactions, and (4) acts as a coolant for the balance mechanism (Brown, 1988).

(c) Sample holders

The holder must allow intimate contact between the sample and its immediate atmosphere, thereby promoting the rapid loss of volatile reaction products. Furthermore, it must be inert to both the sample and the atmosphere, and even if the holder does not react with the sample or products, it may catalyze or inhibit reactions in the sample. The sample should be spread thinly over a wide area on an open plate or shallow dish. Noble metals (e.g. platinum, gold and silver), glass, alumina, silica and porcelain are commonly used as constructional materials for holders. The constructional material of the holder is largely determined by the temperature range of the measurements. The sample holder should have a high thermal conductivity to ensure rapid transfer of heat to the sample, and should be disposable or easily removed for cleaning (Daniels, 1973).

2.1.1.2 Sample characteristics

(a) Sample form

TG samples may be in the form of a powdered solid (either compressed into a pellet or spread thinly over the pan surface), a thin film or a liquid. Powders should be spread thinly over a large open pan, but must not be fine enough to be disturbed by a flowing atmosphere (Daniels, 1973).

(b) Sample weight

The weight of a sample, like its form, may influence the TG curve by affecting diffusion, heat transfer or the accessibility of the atmosphere. Small sample sizes,

usually about 10 mg, are preferred in TG since large samples tend to give poorly resolved curves (Daniels, 1973).

2.1.2 Sources of error in thermogravimetry:

The sources of error in thermogravimetry can lead to considerable inaccuracies in the temperature and weight-loss or weight-gain data obtained.

2.1.2.1 Sample container air buoyancy

This refers to the apparent mass gain that occurs when an empty and thermally inert crucible is heated. This effect is due to thermomolecular flow that occurs when the balance is operating at low pressure. As the sample is heated, the density of the atmosphere around the sample decreases, and the upthrust, caused by the gas, will decrease. The crucible will therefore show an apparent gain in measured mass (Wendlandt, 1964).

2.1.2.2 Furnace convection currents and turbulence

An apparent mass loss is caused by the upper flowing stream of gas in the vicinity of the sample holder. The upper flowing stream can be reduced by changing the configuration of the sample holder. It is also important that the size and shape of the sample crucible are adjusted appropriately. In some cases, it is recommended that a small hole is made in the crucible (Hatakeyama, et al., 1998)

2.1.2.3 Temperature measurements and calibration

The sample temperature, T_s, will usually lag behind the furnace temperature, T_f, and T_s cannot be measured very readily without interfering with the weighing process. The lag, $T_f - T_s$, may be as much as 30 ^oC, depending upon the operating conditions. The lag is more prominent when operating in vacuum, in fast-flowing atmospheres and with high heating rates. Temperature measurement is usually obtained by a thermocouple and it is advisable to have separate thermocouples for the measurement of T_s and for furnace regulation.

An ingenious method of temperature calibration for small furnaces makes use of the Curie points of a range of metals and alloys. On heating a ferromagnetic material, it loses its ferromagnetism at a characteristic temperature known as the Curie point. If a magnet is positioned below the sample of a ferromagnetic material, the total downward force on the sample, at temperatures below the Curie point, is the sum of the sample weight and the magnetic force. The magnetic force is reduced to zero at the Curie point and an apparent mass loss is observed. A multi-point temperature calibration may be obtained by using several ferromagnetic materials (Brown, 1988).

2.1.3 Other errors

The errors that are caused by random fluctuations of the recording mechanism, furnace induction effects, electrostatic effects, changes in thermobalance environment, and so on, can be eliminated by proper thermobalance design, construction and location in the laboratory. Condensation on the cool part of the sample holder support rod is another source of error (Wendlandt, 1964).

2.1.4 Applications of thermogravimetry

The method of TG is basically quantitative in nature in that the mass-change can be accurately determined. However, the temperature ranges in which the mass-changes occur are quantitative in that they depend on the instrumental and sample characteristics. Some of the many applications of TG are listed below (Wendlandt, 1964):

(a) Thermal decomposition of inorganic, organic and polymeric substances.
(b) Corrosion of metals in various atmospheres at elevated temperatures.
(c) Solid-state reactions
(d) Roasting and calcining of minerals
(e) Distillation and evaporation of liquids
(f) Pyrolysis of coal, petroleum and wood
(g) Determination of moisture, volatiles, ash and purity
(h) Rates of evaporation and sublimation

2.2 X-ray Diffraction

X-ray crystallography encompasses a group of techniques which utilise the wave properties of X-rays. The positions and intensities of the X-rays diffracted by a crystalline solid can provide us with a wealth of information such as crystal structure, composition of a solid, particle size, evidence of decomposition, polymorphism, preferred orientation, disorder, and so on (Whitson, 1987).

2.2.1 Generation of X-rays

X-rays are produced when high speed electrons are suddenly stopped by a solid object. The generation of the X-rays needs a source of electrons, a means of accelerating them, and a target to stop them (Whitson, 1987).

X-rays are generated in an X-ray tube. Two varieties are in current use, known as the side window tube and the end window tube.

Figure 2.2 shows a schematic diagram of a side window tube. The electrons are produced by an electrically heated tungsten filament and they are then accelerated towards the target by applying a large potential difference (voltage), e.g. 60 kV, between the filament and the target. To allow free flight of the electrons, the X-ray tube is evacuated to produce a very high vacuum.

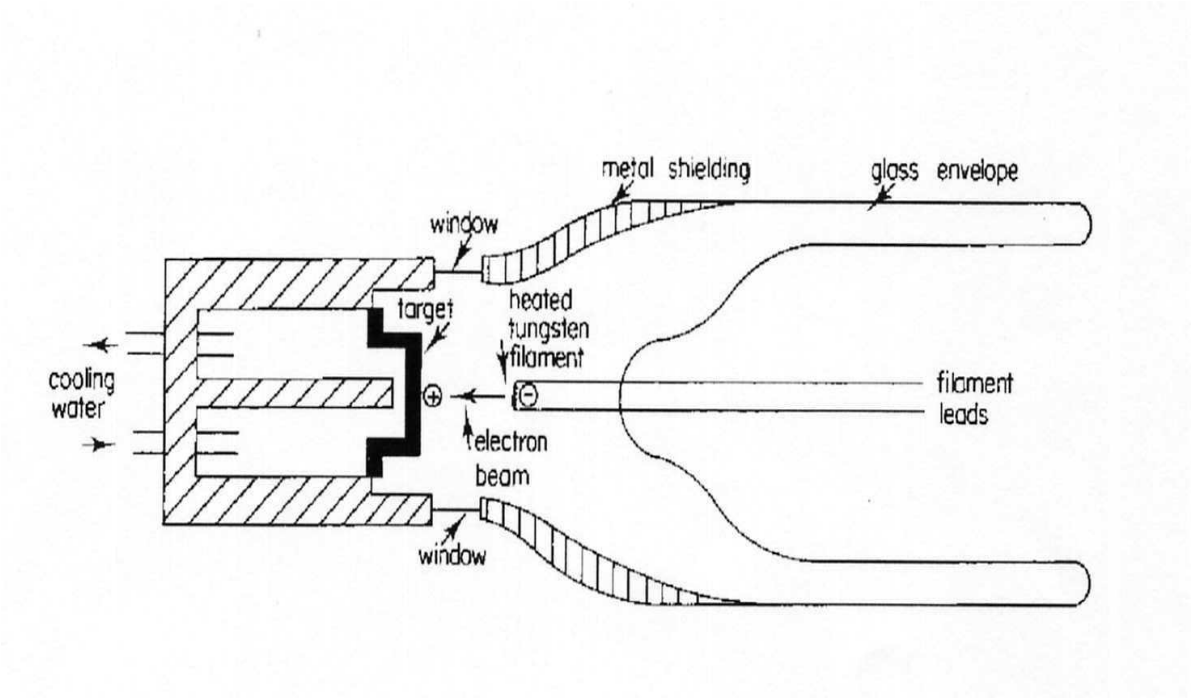

Figure 2.2. Schematic diagram of a side window tube (Whitson, 1987)

The high speed electrons are stopped by the atoms of the target resulting in X-rays being produced in all directions from the surface of the target. Since X-rays are harmful to life, the tube is partly cladded with a heavy absorbing material such as lead. The X-rays are allowed to leave the tube through one or more windows, these being made of a thin light metal such as aluminium or beryllium.

Of the total energy supplied to the tube, only a fraction (about 1 %) is converted to X-rays. Most of the energy is transferred into heat. To prevent the target from melting, it is cooled from behind by running water. The target material is made of a high melting material which has good thermal conductivity. For the production of high intensity X-rays, a target element should have a high atomic number. Typical materials are pure transition metals such as Mo, W, Cu, Cr etc.

2.2.2 The Powder Diffractometer

Figure 2.3 shows the layout of a typical powder diffractometer.

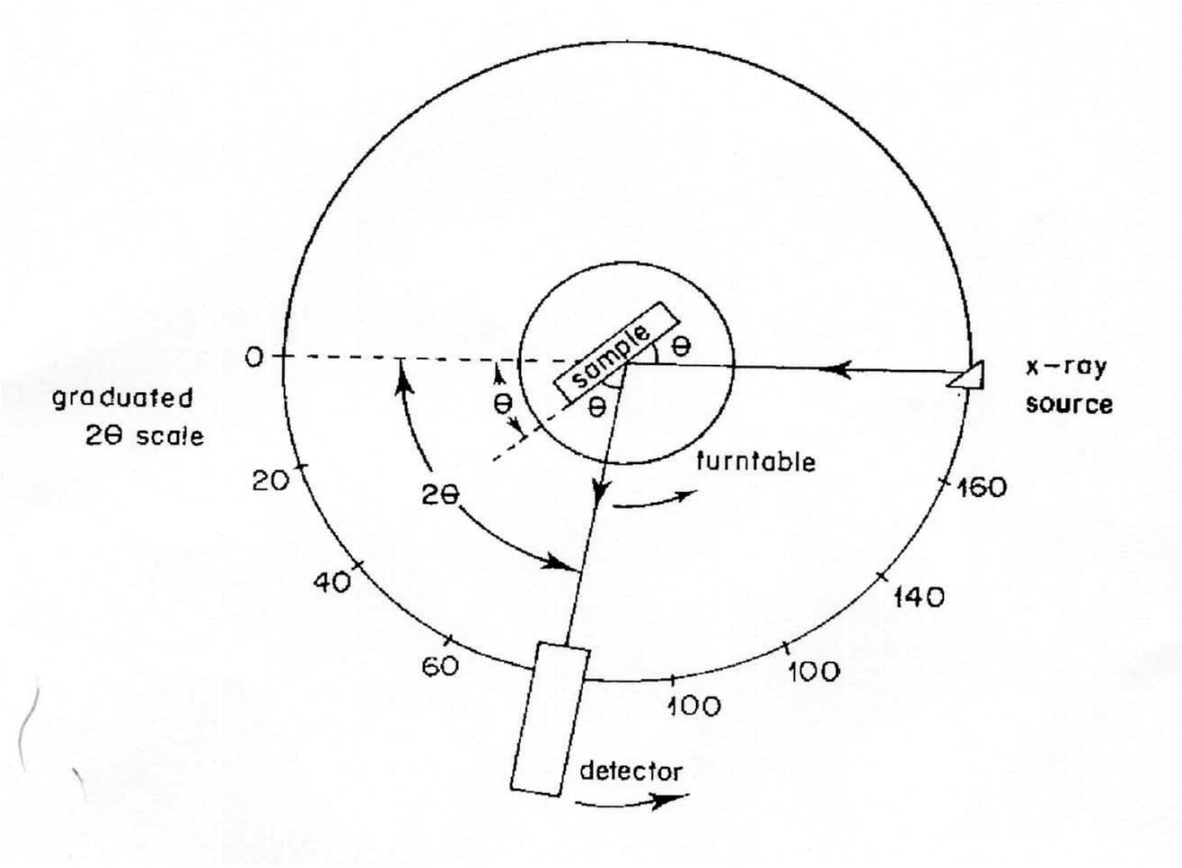

Figure 2.3. Layout of a powder diffractometer (Whitson, 1987)

A flat specimen is mounted on a turntable around which moves the detector. As the sample rotates, so the angle θ between the incident beam and the sample changes and whenever the Bragg condition is fulfilled**,** X-rays are reflected to the detector. The Bragg condition is,

$$\text{Sin } \theta = n\lambda/2d$$

where n is number of planes, λ is wavelength and d the d-spacing**.** The detector is connected to the specimen table and geared in such a way that when the table rotates through θ degrees, the detector rotates through 2θ degrees. This results in the detector always being in the correct position to receive the rays reflected by the sample.

To record a diffraction pattern, the detector is positioned at or near 0^o on the graduated 2 θ angle and is then driven by a motor at constant speed, e.g. 2^o per minute. Alternatively, the detector may be driven clockwise from about 170^o. The X-rays reaching the detector are registered as a series of peaks on top of a background due to white radiation.

Figure 2.4 shows the layout of powder diffractometer and detector circuits. A divergent beam of X-rays is produced from the source (A). The X-rays diffracted by the sample (B) converge to a focus at the slit (C) and enter the detector (D). The detector is an electronic device called a counter, and it converts the X-rays diffracted by the sample into electric pulses in the circuit to which they are connected. The particular circuit used depends on whether the diffractometer is being used in the scanning mode (recording a diffraction pattern) or is in the stationary mode (measuring peak intensity).

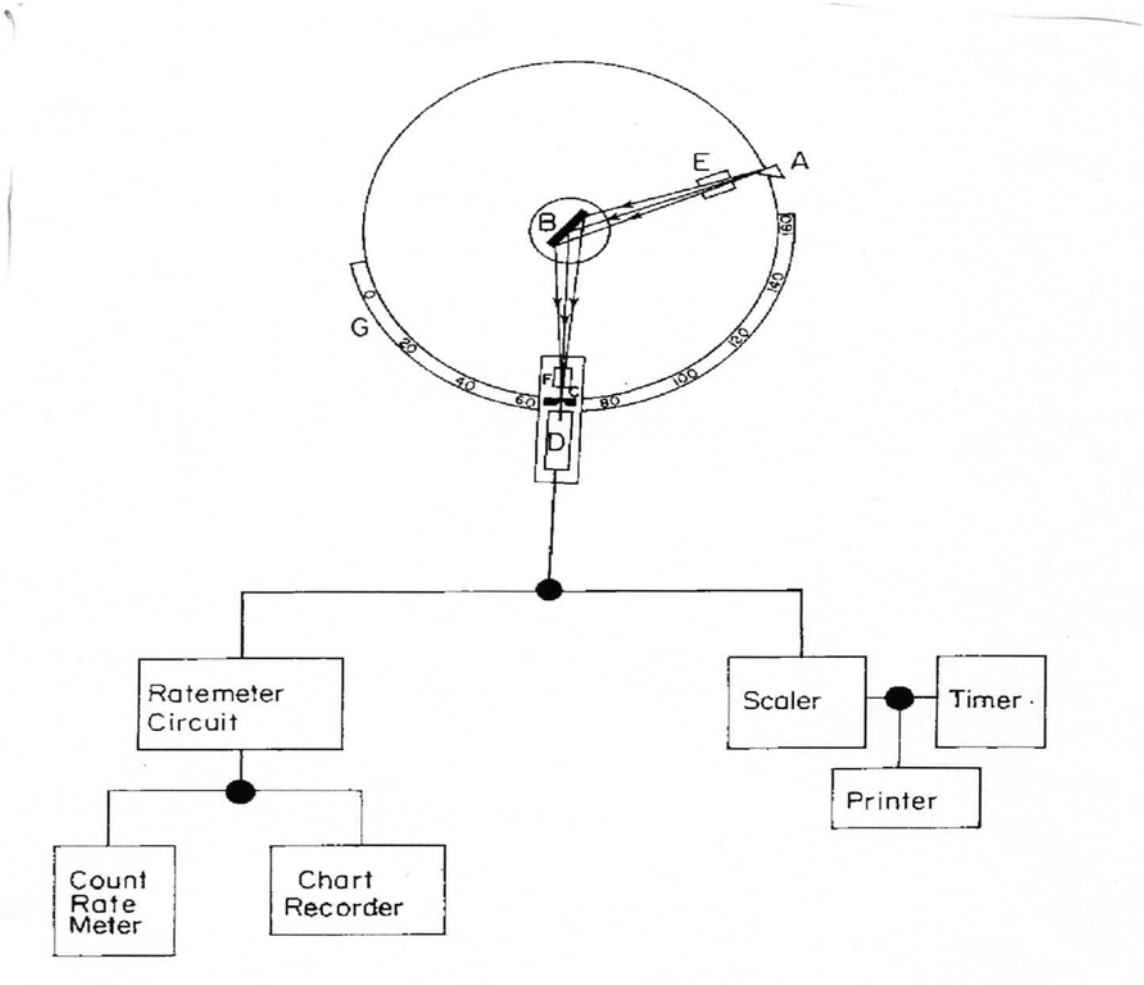

Figure 2.4. Layout of powder diffractometer and detector circuit (Whitson, 1987)

The ratemeter circuit is used for the scanning mode. As the detector rotates, so a succession of pulses gives a steady current which is displayed continuously on the ratemeter. The resulting chart is a record of counts per standard time versus 2 θ. As the detector moves through each degree (or half degree), a pulse is sent to a second pen. Thus the 2 θ scale and the diffraction pattern are recorded at the same time.

When the diffractometer is used in the stationary mode, the pulses of current are counted electronically by the scaler-timer circuit. This gives the average counting rate over a preselected length of time.

XRD is used for both qualitative and quantitative phase analysis. It is used for the determination of unit cell parameters and the study of order/disorder in solids. It is also useful in the study of preferred orientation and the determination of particle size (Whitson, 1987).

2.2.3 Sample preparation for XRD analysis

In order to obtain a satisfactory powder pattern, a crystalline powder must meet certain specifications. The most important factors requiring attention in sample preparation for the diffractometric powder technique are (Verryn, 2003):

(a) Crystallite or grain size
(b) Sample thickness
(a) Preferred orientation
(b) Sample homogeneity
(c) Strain or cold-working (mainly metals)
(d) Surface planarity

2.2.3.1 Preparation of Powders

It is most important that the number of crystallites contributing to each reflection is large enough to generate signals of reproducible intensity, and that preferred orientation of the crystallites are held to a minimum (i.e. total randomness of the crystallite orientation). A sample can also be ground too fine, making it amorphous to X-ray diffraction.

2.2.3.2 Small samples

Sample support and positions become very important if extremely small quantities of samples are to be analyzed. The technique called ZBH (Zero Background Holder) can be used on samples as small as 1.0 mg.

2.2.3.3 Special samples

Slightly reactive, hygroscopic materials, slurries and liquids can be sealed by placing them in a sample holder and covering them with a thin film (e.g. mylar foil) or even cellophane tape (the diffraction pattern of the sealing material must be recorded and subtracted from the sample)

2.2.3.4 Sample Thickness

The sample thickness required is closely linked to the depth of X-ray penetration. Considering a flat specimen, the thickness of the sample must be large enough to give maximum diffracted intensity (in this case ± 99%). A criterion for this condition is

$$\mu t \geq 3.45 * (\rho/\rho') \sin \theta$$

where t is the sample thickness in centimetres, μ and ρ are, respectively the linear absorption coefficient and the density of the solid material composing the powder, and ρ' is the density of the powder including interstices, μ'= (μ/ρ)= mass absorption coefficient

2.2.3.5 Preferred Orientation

Each grain in a polycrystalline aggregate normally has a crystallographic orientation different from that of its neighbours. Considered as a whole, the orientations of all the grains may be randomly distributed in relation to some selected frame of reference, or they may tend to cluster about some particular orientation. Any aggregation characterized by such a condition is said to have a "preferred orientation". This can be greatly reduced through the reduction of the crystallite size. The method of mounting the sample, such as back and side filling can be followed to reduce preferred orientation.

2.3 X-ray Fluorescence

X-ray fluorescence spectrometry (XRF) is a technique for the determination of elemental abundances in samples that are normally presented for analysis in solid

form (liquids can be analysed directly as well, although such applications are not as common). The sample surface is excited by a primary beam of X-ray radiation. Provided they are sufficiently energetic, X-ray photons from this primary beam are capable of ionizing inner shell electrons from atoms in the sample, resulting in the emission of secondary X-ray fluorescence radiation of energy characteristic of the excited atoms. The intensity of this fluorescence radiation is measured with a suitable X-ray spectrometer and, after correction for matrix effects, can be quantified as the element abundance. The technique is notionally claimed to have the potential of determining all the elements in the periodic table from sodium to uranium to detection limits that vary down to μg/g level. However, using specialized forms of instrumentation, this range may be extended for same sample types down to at least carbon, although with reduced sensitivity and with some care required in the interpretation of results, owing to the very small depth within the sample from which the analytical signal originates for this element.

XRF has the capability of determining a range of difficult elements such as S, Cl, and Br that cannot always be detected satisfactorily by other atomic spectrometry techniques. One disadvantage of the technique is that it does not have adequate sensitivity for the direct determination of other key elements (Cd, Hg, Se, for example) at the low concentrations of interest in environmental studies (Smith, et al., 2004).

2.3.1 Production of X-rays

2.3.1.1 Characteristic fluorescence X-rays

A fluorescence X-ray is emitted when an inner shell orbital electron in an atom is displaced by some excitation process such that the atom is excited to an unstable ionized state. In the case of X-ray fluorescence, excitation is achieved by irradiating the sample with energetic X-ray photons from a suitable source. If the irradiating X-ray photon exceeds the ionization energy of the orbital electron, there is a certain probability that the energy of the photon will be absorbed, leading to the ionization loss of the electron from the atom. This process is called the photoelectric effect and is shown diagrammatically in Figure 2.5. Due to the vacancy in the inner electron

orbital, the atom is left in a highly unstable state. Electron transitions occur immediately, whereby the inner shell vacancy is filled by an outer shell electron so that the atom can achieve a more stable energy state.

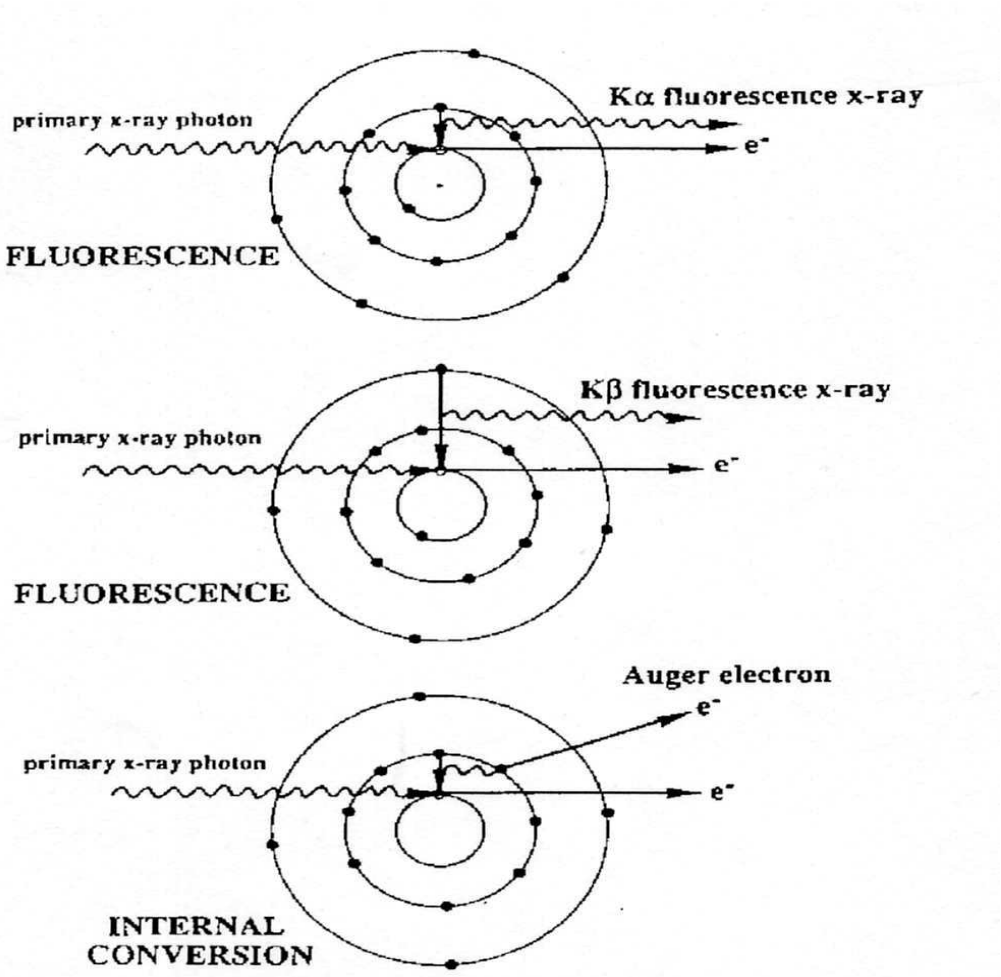

Figure 2.5. Schematic diagrams of the electron transitions that led to the emission of Kα and Kβ fluorescence X-ray photons and an Auger electron (Smith et al., 2004)

2.3.1.2 Continuum Radiation – The X-ray tube

Continuum X-ray radiation is generated when electrons (or protons or other charged particles) interact with matter. Figure 2.6 shows the schematic diagram of both the side window and an end window X-ray tube.

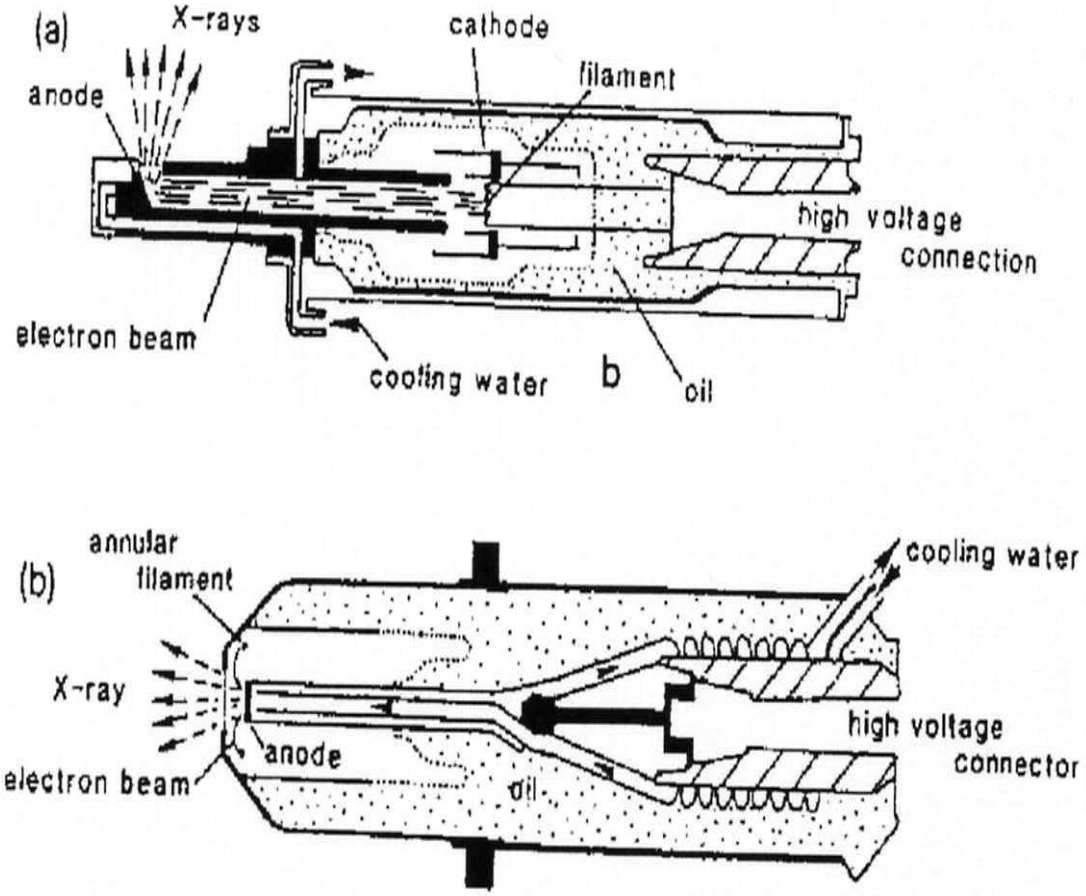

Figure 2.6. Schematic diagrams of (a) side window design of an X-ray tube, (b) end window X-ray tube (Smith et al., 2004)

The X-ray tube consists of a filament, which when incandescent serves as a source of electrons. The electrons are then accelerated through a large potential difference and focused onto a metal target (the anode). When the filament is heated to incandescence by an electric current, thermionic emission of electrons occurs. By applying a large potential difference between the filament and anode (typically 10 – 100 kV), the electrons are accelerated and bombard the anode with a corresponding energy (in keV). Interactions between energetic primary electrons and atoms of the sample result in the following phenomena.

(a) Characteristic Fluorescence Radiation- Incident radiation is capable of

displacing inner shell electrons of atoms of the anode causing the emission of fluorescence X-rays characteristic of the anode material. Commonly used tubes include those having anodes of Rh, Mo, Cr, Sc, W, Au, or Ag.

(b) Continuum Radiation- Incident electrons also lose energy by a repulsive interaction with the orbital electrons of target atoms.

(c) Heat- A considerable amount of heat is dissipated when the electron beam from the filament interacts with the anode.

(d) Backscattered Electrons- A small proportion of the electrons from the primary beam are scattered back out of the surface of the anode.

Figure 2.7 shows the layout of a typical wavelength dispersive spectrometer. An X-ray spectrometer consists of three principal sections (Whitson, 1987):

(a) The specimen chamber- where the sample is excited by a primary X-ray beam,

(b) The monochromator – where the fluorescing radiation is dispersed, and

(c) The detector and associated electronics- where the dispersed radiation is detected, amplified and displayed.

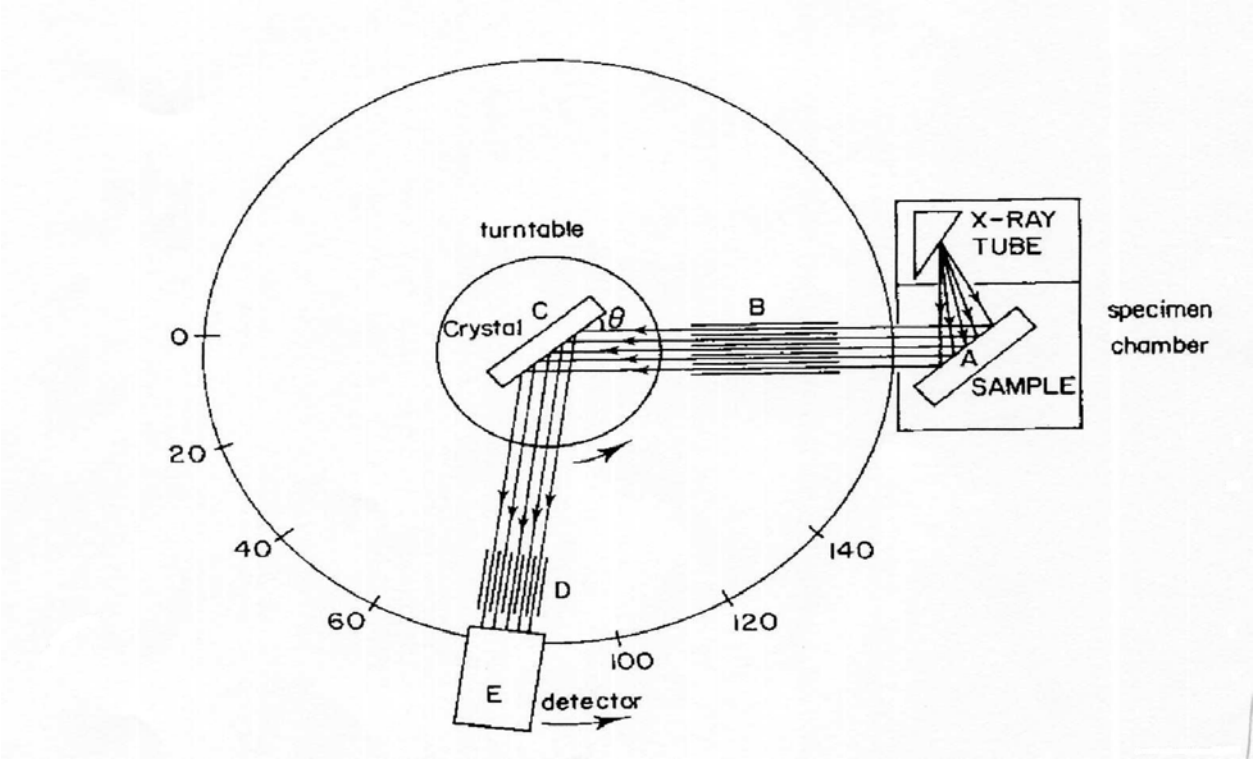

Figure 2.7. Layout of a typical dispersive spectrometer (Whitson, 1987)

The sample (A) is being irradiated by a primary X-ray beam causing it to fluoresce each element emitting its own characteristic X-ray radiation. Part of the radiation is collimated by a system of slits (B) onto an analysing crystal (C). The crystal is mounted on a turntable which can be rotated by a motor. As the crystal rotates, so the angle θ presented to the fluorescent rays changes. Whenever the Bragg Equation is fulfilled for a particular X-ray wavelength, i.e. when Sin θ = nλ/2d, this part of the beam is reflected by the crystal. The reflected beam passes through a set of collimating slits (D) and enters the detector (E).

2.3.2 Types of conventional spectrometers

There are four basic types of instruments:

(a) Manual Spectrometer

It consists of one crystal/collimator/detector system. Although scans for qualitative work are motor driven, for quantitative work all instrument settings (such as tube current and voltage) are made manually. The changing of instrument components such as collimator, analysing crystal or detector is performed manually.

(b) Semi-automatic Spectrometer

It is used when a large number of diverse samples are to be analysed. A semi-automatic instrument is more convenient than a manual one. Here the machine settings and instrument components appropriate to each individual sample are selected by simple operation of push buttons and multi-position switches.

(c) Automatic Sequential Spectrometer

An automatic sequential spectrometer is used for the routine analysis of a large number of similar samples. The spectrometer is usually interfaced with a computer which has been programmed to control the entire sequence of the analysis. This involves control of sample changing, changing of settings and of instrument

components applicable to each element of interest in each sample, moving the spectrometer from one 2θ setting to another, collection of intensity data, and calculation of elemental concentration.

(d) Simultaneous Automatic Spectrometer

Simultaneous automatic spectrometers are also suited for the routine analysis of a large number of samples. These instruments consist of up to 26 single channel instruments situated around the X-ray tube and sample. Each channel is fixed at the 2θ angle of a specific element, and each channel is fitted with instrument components most suited for that element. The intensities are collected from each channel and fed to a computer for the calculation of elemental concentrations.

2.3.3 Qualitative analysis

The spectrometer is used in the scanning mode for qualitative analysis whereby it rotates through a definite 2θ range, of 10^{o} to 145^{o}. X-rays reaching the detector are registered, the signals amplified and displayed as a series of peaks referred to as lines.

For a particular analysing crystal, the line-to-2θ tables list the wavelength and 2θ values of the characteristics elements that can be dispersed by the crystal. The data are listed in order of increasing atom number. 2θ-to-line tables list similar data, but in increasing magnitude of 2θ. The interpretation of an XRF trace involves reading off the 2θ values of the peaks and then 2θ-to-line tables, applicable to the analysing crystal used.

2.3.4 Quantitative analysis

The amount of a particular element present in a sample related to the intensity of any one of the element's characteristic lines. The spectrometer is used in the stationary mode for quantitative work whereby the crystal is fixed at the appropriate angle to reflect one of the element's characteristic lines, the detector automatically being in the correct position to receive it. The spectrometer can then be adjusted to another angular setting and the procedure repeated for the next element of interest. The actual

intensity is displayed either in terms of the number of counts per preset time, or the time to accumulate a preset number of counts, say 10000. The intensity value is used to determine the element's concentration in the sample

2.3.5 Sample preparation for XRFS

The preferred forms of sample preparation for quantitative analysis include a solid disk prepared by compressing powdered material, a glass disk prepared after fusion of a powdered sample with a suitable flux, loose powder placed in an appropriate sample cup, and dust analysed in situ on the collection filter (Smith, et al., 2004).

(a) Pressed Powder Briquettes

Pressed pellets are usually prepared for trace elements. The powders are mixed with a suitable binder (e.g. Somar mix, Sugar and Hoechst wax) and pressed at ± 70 tons/in^2 (Loubser, 2005).

(b) Fused Beads

This technique is mostly used for major element analysis, as the sample is diluted by the flux (e.g. $LiBO_2$, $Li_2B_4O_7$) and this would increase the detection limit for trace elements. A heavy absorbing element like Na_2CO_3 is sometimes added to all samples and standards to minimise matrix effects. The samples are fused at 1100 ^oC in a muffle furnace or over a gas burner, before being cast in a Pt/Au 5% casting dish. Some of the many advantages of using fused beads are homogeneous mixtures, no particle and mineralogical effects. The matrix effects or the interferences within the sample are diluted and a flat mirror surface is obtained.

2.4 Surface area analysis

The specific surface area of a solid is one of the first things that must be determined if any detailed physical and chemical interpretation of its behaviour as an adsorbent is to be possible. Each method for surface area determination involves the measurement of

some property that is observed qualitatively to depend on the extent of surface development and can be related by means of theory to the actual surface area (Adamson, 1990).

The most important methods for specific surface area analysis of solids are based on adsorption. The following two assumptions are made (Mikhail et al., 1983):

(a) It is possible to determine the quantity of adsorbate required for complete coverage of the substrate surface by a monolayer, and

(b) The cross-sectional area of an adsorbed molecule is known and independent of the substrate (adsorbent).

Solid surfaces in contact with a gas (or solid) will adsorb molecules. Forces controlling this process may be of chemical (chemisorption) or physical nature (physisorption). Chemisorption occurs in one layer only and the reaction is not readily reversible because the molecules react with the sample surface. In physisorption, the adsorbed gas molecules are held to the surface by weak (van der Waals) forces and the process is easily reversed by raising the sample temperature. The interaction between the adsorptive and the adsorbent can take several forms, and is dependent on the interaction between solid and gas molecules and on the nature of the sample (Porous or non-porous).

2.4.1 Physical adsorption of gases

Surfaces of solids to be characterized by physical adsorption of gases must be cleaned of previously adsorbed (physisorbed) material. In most cases this will mainly be water, which is strongly adsorbed on most materials. The surfaces of the samples are cleaned by treating them at elevated temperatures to speed up the cleaning process. By applying vacuum or flowing inert gas over the sample for some period, the adsorbed molecules are removed. The nature of the adsorbed molecules and the pore structure of the sample govern the time needed to effectively clean the sample. The temperature should be high enough to speed up the cleaning, without changing the sample physically or chemically in any way. The time needed may be established by checking the relation between time and measured result. After some preparation time,

no further increase in the resulting surface area will be observed. This combination of temperature and time are the optimal outgas conditions (Muller, et al., 1997).

The most widely employed technique for the determination of surface area by gas adsorption is the physical adsorption of nitrogen at a low temperature (the boiling point of liquid nitrogen). Adsorption isotherms are usually constructed by measuring the uptake of gas (adsorptive) at increasing partial pressure over the sample (adsorbent) (Muller, et al., 1997).

2.4.2 BET theory

Brunaer, Emmett and Teller (BET), made a significant advance in the interpretation of the physical adsorption process. Starting with the basic concepts of Langmuir, these authors assumed that the rate of evaporation from the nth adsorbed layer was equal to the rate of condensation of the (n-1)th layer. From this assumption it proved possible to derive the BET equation (Hair, 1967).

The BET theory results in the following equation which describes the isotherm:

$$\frac{P/P_O}{V_a\left(1-P/P_o\right)} = \frac{1}{V_m C} + \frac{C-1}{C}\frac{P/P_o}{V_m}$$

where V_a is the volume adsorbed at pressure P and absolute temperature T, P_o is the vapour pressure of the gas at temperature T, V_m is the volume of gas adsorbed when the adsorbent surface is covered with a unimolecular layer and is termed the monolayer (Mikhail et al., 1983). The factor C represents the B.E.T. constant and is related to the heat of adsorption (enthalpy) at the first adsorbed layer. It describes how strong the adsorbate molecules are attracted to the adsorbent surface. Its value for surface area results to be reliable, should be between 20 and 200. A low number represents strong adsorbate-adsorbent interaction. C values larger than 200 indicate very intensive interaction between adsorbate and adsorbent. In those cases the interaction is so strong that not just monolayer-multilayer adsorption is occurring, but possibly micro pore filling is taking place (Muller, et al., 1997). If the function

$$\frac{\left(P/P_o\right)}{V_a\left(1-P/P_o\right)}$$

is plotted against P/P_o , a straight line should result, the slope and intercept of which give the values of V_m and C, respectively (Mikhail et al., 1983).

The BET theory concentrates on the forces binding the adsorbate to the adsorbent surface. The existence of such forces, however, implies that they should also attract the adsorbate molecules laterally (Mikhail, et al., 1983).

The specific surface area of non-porous solids is estimated from the physical adsorption of gases. The monolayer capacity of the adsorbent is calculated from the adsorption isotherm. It is defined as the quantity of the adsorbate which can be accommodated in a completely filled, single layer of molecules (a monolayer) on the surface of the solid. The specific surface area, S (m^2/g), is directly proportional to the monolayer capacity with the relationship between the two being given by the simple equation,

$$S = \frac{X_m N}{M 10^4} A_m \, x10^{-16}$$

$$= \frac{X_m}{M} N A_m \, x10^{-20}$$

where X_m is the monolayer capacity in grams of adsorbate per gram of solid and M is the molecular weight of the adsorbate. A_m is the area in square Angstrom units occupied per molecule of adsorbate in the completed monolayer, hence the appearance of the factor 10^{-16} (Gregg et al., 1967).

In this study the Nova 1000e Surface Area & Pore Size Analyzer was used for the measurement of the surface area of the samples. The instrument measures the surface area of granulated and powdered solids or porous materials, by determining the quantity of a gas that adsorbs as a single layer of molecules, a so-called monomolecular layer, on a sample. This adsorption is done at or near the boiling point of the adsorbent gas. Under specific conditions, the area covered by each gas

molecule is known within relatively narrow limits. The area of the sample is thus directly calculable from the number of adsorbed molecules, which is derived from the gas quantity at the prescribed conditions and the area occupied by each. The instrument permits the measurement of surface areas by single point or multipoint procedures. Measurements for this study were performed using the single point determination method. For nitrogen the value of C is usually sufficiently large to warrant the assumption that the intercept in the BET equation is zero. Thus, the BET equation in Section 2.4.2 reduces to (Nova Operation Manual, 2002),

$$W_m = W\left(1 - p/p_o\right)$$

By measuring the amount of nitrogen adsorbed at one relative pressure (preferably near p/p_o = 0.3) the monolayer capacity W_m can be calculated using the above equation and the ideal gas equation,

$$W_m = \frac{PVM}{RT}\left(1 - P/P_O\right)$$

The total surface area then can be obtained from the equation below,

$$S_t = \frac{W_m N A_{cs}}{M}$$

That is,

$$S_t = \frac{PVNA_{cs}\left(1 - P/P_O\right)}{RT}$$

CHAPTER 3

EXPERIMENTAL

3.1 Materials

All chemicals used were of analytical grade, with the exception of solid magnesia (MgO) and the distilled water that was used for solutions. The magnesia used in this investigation was obtained from the calcination of highly reactive magnesia (caustic magnesia) in an electric furnace at 1200 ^{o}C for 1 hour using high temperature crucibles. The calcined magnesia was of an intermediate quality between medium and hard-burnt magnesia (Section 3.3) with a BET-measured surface area of 5.0 m^2/g. The highly reactive magnesia (caustic magnesia) was supplied by Chamotte Holdings (PTY) LTD, a mining company in South Africa. It had been produced by the calcination of natural magnesite mineral ($MgCO_3$) between 800 ^{o}C and 900 ^{o}C in an electric rotary kiln for approximately 30 minutes. The specific surface area of the reactive magnesia was 73.48 m^2/g.

3.2 Hydration procedure

The following procedure was followed to study the effect of each hydrating agent on the hydration of magnesium oxide.

A 35.0 g sample of calcined magnesite (as obtained from the supplier) was calcined at 1200 ^{o}C for 1 hour. The sample was allowed to cool to room temperature. It was hand ground with a porcelain mortar and pestle to break the large lumps and then milled for 30 seconds with an Ika electric mill. The sample was then sieved for 5 minutes to a particle size of less than 75 μm with an Electromagnetic Sieve Shaker EMS-8. To hydrate the MgO, 10 g of the calcined sample was stirred at a constant rate of 250 rpm in a 100 ml of a 0.1 M hydrating solution, while the temperature was controlled by performing the reaction in a water bath at temperatures ranging between 30 ^{o}C and

80 ^{o}C for 30 minutes. The hydrating agents used were ammonium chloride, magnesium acetate, magnesium nitrate, nitric acid, acetic acid, water, magnesium chloride, sodium acetate and hydrochloric acid. The pH values of the solutions before the addition of MgO are shown in Table 3.1. The hydration experiments were repeated twice for all the hydrating agents and the average percentage of magnesium hydroxide was reported. The pH and temperature were measured simultaneously at one minute time intervals with a pH 510 pH/mV/^{o}C meter from Eutech Instruments. The stirrer was stopped at 25 minutes to allow for the solids to settle for better filterability.

At the end of each experiment, the slurry was vacuum filtered. The solids remaining in the filter, were washed twice with 50 ml water, dried at 200 ^{o}C for 2 hours and then hand ground with a porcelain mortar and pestle. The degree of hydration was determined by TG analysis.

The acidic hydrating agents were chosen because the MgO solubility is increased with an increase in H^{+} concentration. The bases were chosen as hydrating agents to gain more insight into the dissolution and hydration steps on the alkaline side of the pH scale (Jost et al., 1997). Literature indicated that in strong basic regions, above pH 12, the degree of hydration greatly decreases because of the high OH^{-} concentration in the solution. The Mg containing compounds were chosen because literature indicated that a rapid and complete hydration requires a high content of Mg^{2+} ions in the aqueous solution, especially in acid regions (Jost, et al., 1997).

Table 3.1. Initial pH values before addition of MgO

Temperature, ^{o}C	NH_4Cl	$(CH_3COO)_2Mg.4H_2O$	$Mg(NO_3)_2$	HNO_3	CH_3COOH	H_2O	$MgCl_2.6H_2O$	CH_3COONa	HCl
30	6.06	8.06	8.08	1.13	3.11	7.40	7.94	8.69	0.86
40	6.08	8.07	7.99	1.14	3.10	7.58	7.81	8.56	0.93
50	5.98	7.93	7.86	1.01	3.09	7.88	7.65	8.76	0.97
60	4.56	7.78	7.54	1.04	2.82	8.04	7.42	8.79	0.88
70	5.20	7.72	7.34	0.91	2.84	8.01	7.25	8.49	0.88
80	4.99	7.63	7.26	0.56	2.90	8.22	7.29	8.30	0.83

3.3 Citric acid reactivity test

The reactivity of the magnesium oxide samples used in this investigation was determined by the industrially used citric acid reactivity test. In this test, 100 ml of a 0.4 N citric acid solution containing 5 drops of phenolphthalein indicator is added to 2.0 g of powdered magnesium oxide. The mixture is shaken until the color changes from white to pink. The time in seconds needed to completely neutralize the acid is then reported as the citric acid reactivity. The reactivity of magnesium oxide can be described by the citric acid reactivity test as set out in Table 3.2 below (Van der Merwe, et al., 2004).

Table 3.2. **Citric acid reactivity test values**

Type of MgO	**Citric acid reactivity test values (Seconds)**
Soft-burnt	< 60
Medium-burnt	Between 180 and 300
Hard-burnt	> 600
Dead-burnt	> 900

Literature also describes an acetic acid reactivity test to determine the reactivity of MgO. In this test, the activity is determined by reacting 5.0 g of magnesia (particle size < 63μm) with 100 ml of a 1 M acetic acid solution. The activity value, expressed as the time needed to completely neutralize the acid, is taken as a measure of the solid reactivity (Birchal, et al., 2000).

3.4 Instrumentation

A Q500 TGA from TA Instruments was used to perform the thermogravimetric analyses. For all the analyses, a heating rate of 10 ^{o}C/min was used under a N_2 atmosphere. Platinum pans were used and the sample masses were approximately 10 mg.

The X-ray fluorescence analyses were performed on an ARL9400XP + spectrometer. The samples were ground to < 75 μm in a tungsten carbide milling vessel, roasted at 1000 ^{o}C to determine the loss on ignition value and after adding 1 g sample to 6 g $Li_2B_4O_7$ fused into a glass slide. Major element analyses were executed on the fused bead.

X-ray powder diffraction analyses were done on an automated Siemens D-501 spectrometer with a 40-position sample changer and monochromated Cu Kα radiation. The samples were prepared using standard Siemens sample holders and the powdered samples were pressed into the holder using a glass slide.

A Nova 1000e Surface Area and Pore Size Analyzer, using nitrogen gas as an adsorbent, was used to determine the surface areas of both MgO and the products.

CHAPTER 4

RESULTS AND DISCUSSION

4.1. Characteristics of the magnesia sample

Some of the physical properties of the calcined and milled MgO used in this study are summarized in Table 4.1

Table 4.1. Properties of calcined MgO

Property	**Value**
Loss On Ignition, %	0.01
Specific surface area, m^2/g	5.04
Citric Acid Reactivity, s	Between 310 and 590
Particle size, μm	<75

The chemical analysis of both the calcined magnesite (as obtained from Chamotte) and the calcined MgO, as determined by XRF, is shown in Table 4.2. The chemical analysis shows that the calcined magnesium oxide consisted mainly of magnesium oxide. The calcined magnesite had a loss on ignition value of 8.63 % wt, which indicates that absorption of CO_2 to form $MgCO_3$ and hydration to magnesium hydroxide had taken place. This was confirmed by XRD analysis (Table 4.3). The calcined MgO contains 95% wt magnesium oxide and it could be considered a relatively pure mineral.

Table 4.2. XRF analysis of calcined MgO and magnesite

Composition	**% wt** Calcined MgO	**% wt** Calcined Magnesite (As obtained from Chamotte)
SiO_2	3.41	3.08
TiO_2	0.00	0.00
Al_2O_3	0.13	0.09
Fe_2O_3	0.28	0.23
MnO	0.02	0.01
MgO	94.70	86.50
CaO	1.08	1.01
Na_2O	0.03	0.09
K_2O	0.01	0.01
P_2O_5	0.01	0.01
Cr_2O_5	0.02	0.01
NiO	0.25	0.22
V_2O_5	0.00	0.00
ZrO_2	0.00	0.00
LOI	0.01	8.63
Total	99.95	99.89

Table 4.3 and figures A1-A2 (Appendix) show the quantitative XRD analysis and XRD spectra (Appendix) of the calcined MgO and calcined magnesite (as obtained from Chamotte) respectively. XRD analyses confirmed that the samples consisted mainly of periclase (MgO). XRD also detected 7.26 % brucite in the calcined magnesite sample and a small amount of quartz which was confirmed by XRF analyses. After laboratory calcination at 1200 ^{o}C for 1 hour, the brucite content of the calcined magnesite (as obtained from Chamotte) decreased from 7.28 to 0.45%. A very small amount of both magnesite and quartz were detected after calcination.

Table 4.3. XRD analyses of MgO

	Calcined MgO	**Calcined Magnesite**
$Mg(OH)_2$ (Brucite)	0.45±0.45%	7.26±0.93%
$MgCO_3$ (Magnesite)	0.86±0.66%	2.13±0.66%
MgO (Periclase)	98.34±0.81%	88.46±1.20%
SiO_2 (Quartz)	0.35±0.18%	2.15±0.51%

The citric acid test for reactivity of the calcined magnesite sample (as obtained from Chamotte) gave a reactivity value of 14 seconds, which corresponds to the value given for a soft-burnt MgO. After calcination at 1200 ^oC for 1hour, reactivity values between 310 and 590 seconds were obtained. These values correspond to MgO of intermediate reactivity, between medium and hard-burnt (Van der Merwe, et al., 2004).

4.2 Thermogravimetric Analysis

Thermogravimetric analyses were conducted using a TGA Q500 from TA instruments in a N_2 flow between room temperature and 600 ^oC at a heating rate of 10 ^oC/min. Accurately weighed samples (*ca*. 10mg) were analysed in Pt pans. Figure 4.1 shows a typical TGA thermogram of the MgO-$Mg(OH)_2$ sample in a N_2 atmosphere. The amount of $Mg(OH)_2$ in the MgO-$Mg(OH)_2$ sample was determined by obtaining curves of mass (%) and derivative mass (% $^oC^{-1}$) against temperature (^oC). One major stage of weight loss was observed for the magnesium hydroxide sample. The first small weight loss at 25 ^oC to about 150 ^oC resulted from loss of moisture. The raw material consisted of MgO, small amount of $Mg(OH)_2$ and $MgCO_3$. The second large weight loss observed in the range 200 ^oC to 400 ^oC, indicated the decomposition of $Mg(OH)_2$ to MgO**.** The weight loss at about 550 ^oC was due to the decomposition of the traces of carbonate present in the sample. The percentage mass loss due to the decomposition of magnesium hydroxide was determined by dividing the experimental mass loss obtained for a specific sample by the theoretical mass loss for the

decomposition of pure $Mg(OH)_2$ (Van der Merwe, et al., 2004). The theoretical mass loss of magnesium hydroxide is 30.9 %.

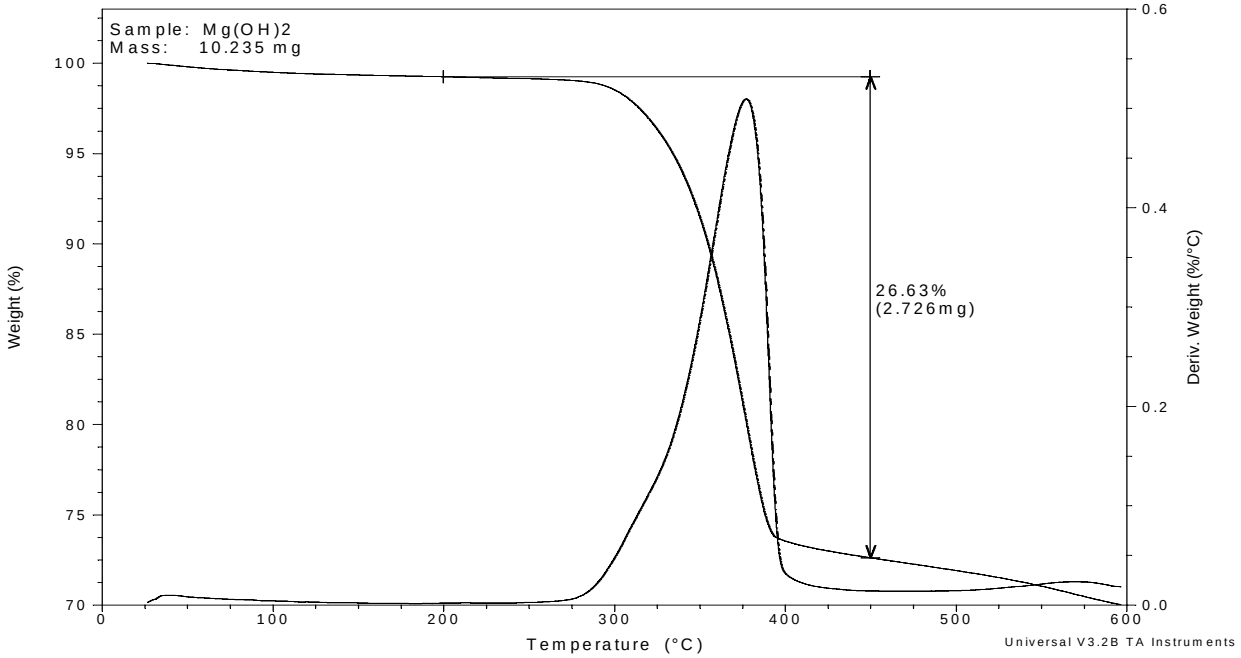

Figure 4.1. A typical TGA thermogram of a MgO-$Mg(OH)_2$ sample

4.3 Variation of degree of hydration with hydration temperature and hydrating agents

Figure 4.2 and Table 4.4 depict the percentage magnesium hydroxide formed as a function of temperature for the different hydrating agents. The hydration at 30 ^oC showed a very small amount of hydroxide being formed. The lowest was 1.2 % in sodium acetate followed by ammonium chloride and magnesium chloride with 1.3 and 1.8 % respectively. A relatively higher percentage was observed in nitric acid with 2.9 %.

At 40 ^oC, sodium acetate and ammonium chloride formed the lowest amount of magnesium hydroxide. The hydrations done in magnesium nitrate and nitric acid formed more hydroxide than those performed in other hydrating agents. The highest percentage was achieved in magnesium nitrate with 4.8 %.

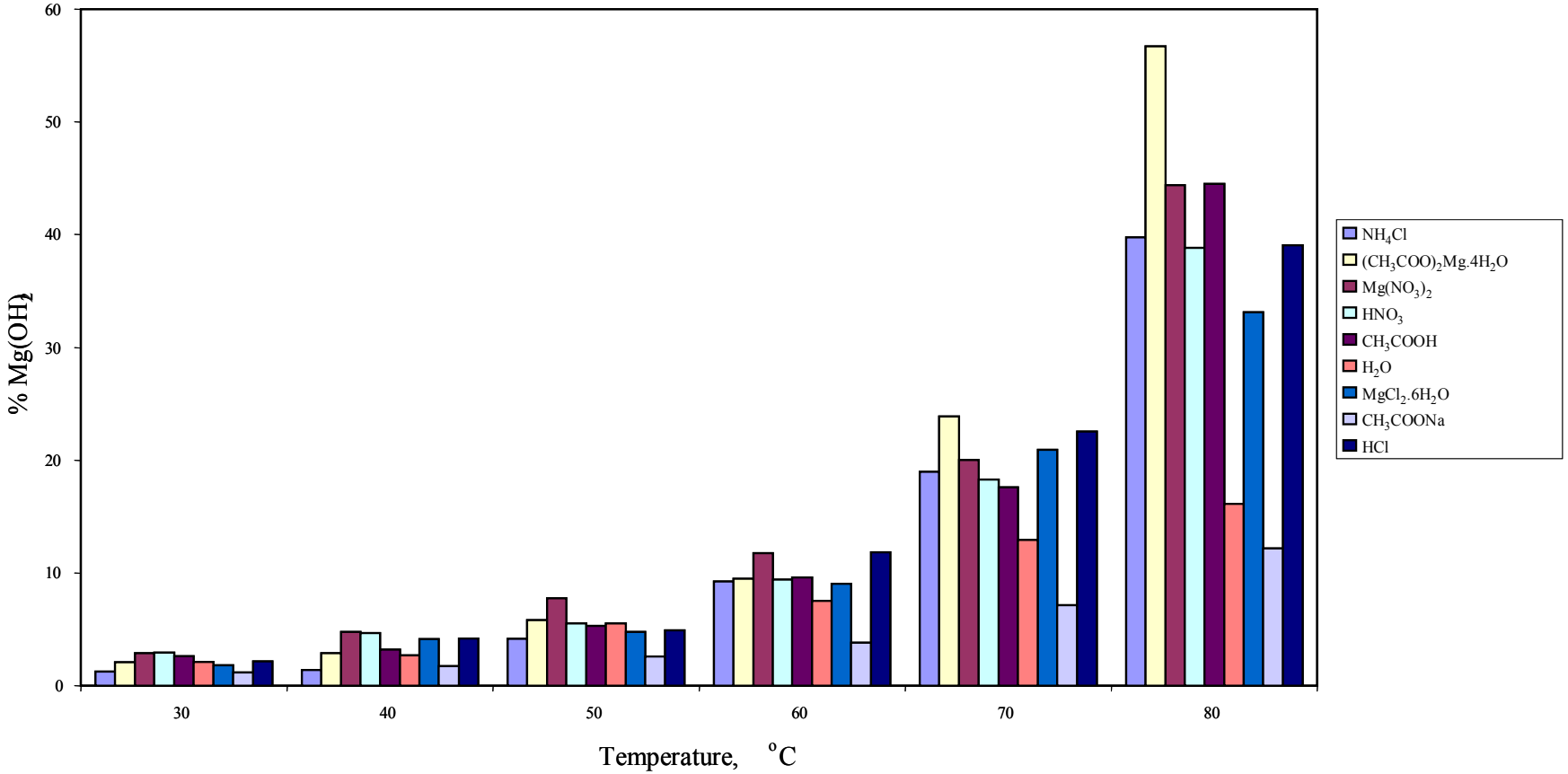

Figure 4.2 The degree of hydration as a function of temperature for the different hydrating agents

Table 4.4. Percentage of $Mg(OH)_2$ formed as a function of temperature

Temperature, ^oC	NH_4Cl	$Mg(CH_3COO)_2.4H_2O$	$Mg(NO_3)_2$	HNO_3	CH_3COOH	H_2O	$MgCl_2.6H_2O$	$NaCH_3COO$	HCl
30	1.3	2.1	2.8	2.9	2.6	2.1	1.8	1.2	2.2
40	1.4	2.9	4.8	4.7	3.2	2.7	4.1	1.8	4.2
50	4.2	5.8	7.8	5.5	5.3	5.5	4.8	2.6	4.9
60	9.3	9.5	11.8	9.4	9.6	7.5	9.0	3.8	11.8
70	19.0	23.9	20.0	18.3	17.6	12.9	20.9	7.2	22.5
80	39.7	56.7	44.4	38.8	44.5	16.1	33.1	12.2	39.1

At 50 ^{o}C, magnesium nitrate formed the largest percentage of magnesium hydroxide (7.8 %) and sodium acetate the least (2.6 %). All other hydrating agents behaved similarly, with the percentage magnesium hydroxide being formed ranging between 4.2 and 5.8 %.

At 60 ^{o}C, sodium acetate resulted in 3.8 % of the hydroxide being formed followed by water and magnesium chloride with 7.5 and 9.0 % respectively. Ammonium chloride, magnesium acetate, nitric acid and acetic acid gave similar results (9.0-9.6 %) while an optimum amount was obtained upon hydration in hydrochloric acid and magnesium nitrate with 11.8 % magnesium hydroxide being formed.

A considerable increase in the amount of magnesium hydroxide obtained from the hydrations performed at 70 ^{o}C was observed. The lowest percentage obtained was in sodium acetate with 7.2 % while water and acetic acid had 12.9 and 17.6 % respectively. The highest conversion level was obtained from the hydration performed in magnesium acetate with 23.9 % magnesium hydroxide. Hydrochloric acid formed more hydroxide when compared to the hydrations done in nitric acid and acetic acid. The hydrations done in ammonium chloride, magnesium nitrate and magnesium chloride gave approximately the same results.

The hydrations at 80 ^{o}C resulted in an optimum amount of the hydroxide being formed when compared to hydrations at 70 ^{o}C. The lowest amount of magnesium hydroxide was obtained in sodium acetate with 12.2 %. Hydration in magnesium nitrate and acetic acid resulted in the same amount of hydroxide being formed. Approximately the same amounts of the hydroxide were also obtained from the hydrations performed in ammonium chloride, nitric acid and hydrochloric acid. The highest percentage of magnesium hydroxide was obtained in magnesium acetate with 56.7 %.

The optimum amount of the magnesium hydroxide formed at higher temperatures is possibly due to the better solubility of the MgO at these higher temperatures. It seems that an increase in temperature increases the solubility of MgO and therefore the precipitation of magnesium hydroxide is high. Literature indicates that the MgO

solubility is high at high temperatures and the magnesium hydroxide solubility is reduced as the temperature is increased (Rocha, et al., 2004).

The increase in the degree of hydration for the hydration performed in magnesium acetate is possible due to the higher concentration of magnesium ions in solution, which precipitate out as magnesium hydroxide (common ion effect). It has also been reported that magnesium acetate is the most soluble of the compounds in the slurry giving Mg^{2+} and acetate ions (Strydom, et al., 2005). The presence of Mg^{2+} ions accelerates the rate of reaction (Van der Merwe, et al., 2004).

The hydration mechanism proposed by Filippou et al (2004) provides an explanation for the enhanced degree of hydration in magnesium acetate solutions. The magnesia particles first dissolve to give magnesium–acetate complex ions, the complex ion then migrates away from the mother particle to give a precipitate of magnesium hydroxide in the bulk of the solution. Filippou et al (2004) suggested that the acetate ions play a crucial role in enhancing the degree of hydration, possibly due to its relatively strong complexation power.

The increase in the amount of magnesium hydroxide produced from hydration in magnesium acetate can also be explained by the hydrolysis of the acetate. A possible mechanism is given below:

(1) Ionization of magnesium acetate:

$$Mg(CH_3COO)_2(aq) \rightarrow Mg^{2+}(aq) + 2CH_3COO^-(aq),$$

where additional Mg^{2+} ions are formed

(2) Hydrolysis of the acetate ion takes place:

$$2CH_3COO^-(aq) + 2H_2O(\ell) \rightarrow CH_3COOH(aq) + 2OH^-(aq),$$

where more OH^- ions are generated

(3) The OH^- ions are removed from solution by Mg^{2+} to form sparingly soluble $Mg(OH)_2$:

$$Mg^{2+}(aq) + 2OH^-(aq) \rightarrow Mg(OH)_2(s)$$

(4) The acetic acid then reacts with MgO to form $Mg(CH_3COO)_2$ and the above series of reactions take place, over and over, each cycle leading to more production of $Mg(OH)_2$.

Consequently, the total magnesium hydroxide formed when magnesium acetate is used as hydrating agent comes from two sources:

(1) From the hydrolysis of the acetate and the subsequent reaction of OH^- ions with Mg^{2+}, and

(2) From the reaction of acetic acid with MgO to produce fresh $Mg(CH_3COO)_2$

4.4 Comparison of the properties of different hydrating agents

The hydration behaviour of nitric acid, hydrochloric acid, acetic acid and water are compared in Figure 4.3. The initial pH values of hydrochloric acid and nitric acid before the addition of magnesium oxide are similar (see Table 3.1). Acetic acid had initial pH values higher than those of hydrochloric acid and nitric acid. The figure shows that all the hydrating agents produced less than 10 % of magnesium hydroxide up to 50 ^oC. At 60 ^oC and 70 ^oC, hydrochloric acid was a good hydrating agent when compared to nitric acid and acetic acid. At 80 ^oC, acetic acid formed the largest percentage of magnesium hydroxide**.**

All the hydrating agents were more effective hydrating agents than water. Hydrochloric acid and nitric acid behaved similarly up to 80 ^oC. It seems that the dissolution of MgO is increased by increase in H^+ concentration, and therefore a higher degree of hydration is obtained in the acidic solutions.

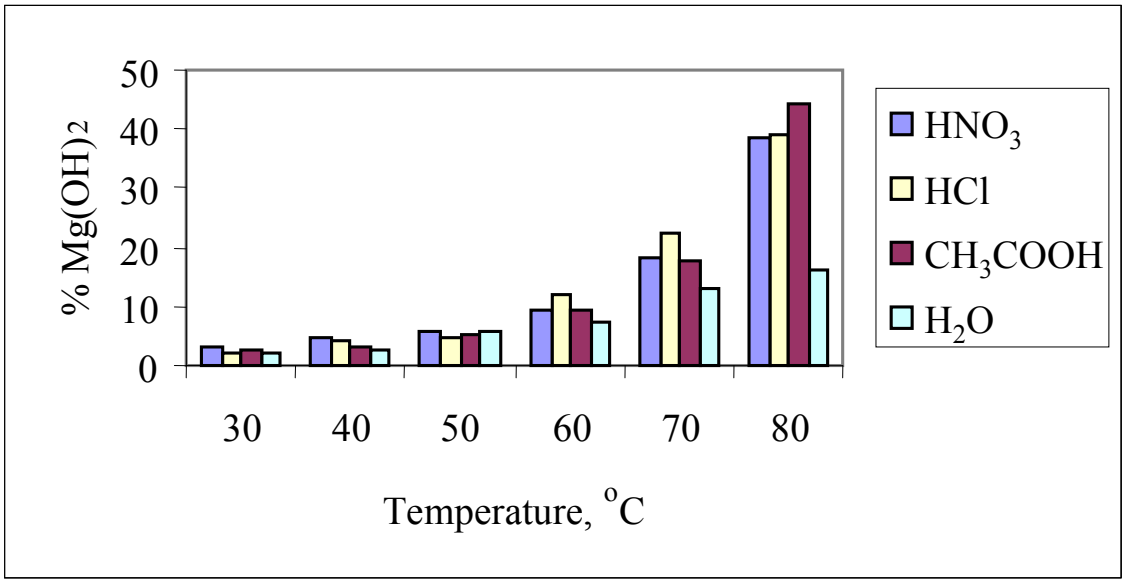

Figure 4.3. Effect of HNO_3, HCl, CH_3COOH and H_2O on the degree of hydration

Sodium acetate, acetic acid, magnesium acetate and water are compared in Figure 4.4. The figure indicates that sodium acetate was the least effective hydrating agent at all temperatures. None of the hydrating agents played a significant role in increasing the degree of hydration up to 60 ^oC. At 70 ^oC and 80 ^oC, a large percentage of magnesium hydroxide was formed in magnesium acetate while acetic acid formed a larger amount of magnesium hydroxide than sodium acetate and water. Water performed better than sodium acetate at all temperatures.

The mechanism of hydration in magnesium acetate described by Filippou et al (2004) provides an explanation for the enhanced degree of hydration in magnesium acetate, and this mechanism can also be used to describe the increase in the degree of hydration when acetic acid is used as a hydrating agent. The additional Mg^{2+} ions in magnesium acetate enhanced the degree of hydration even more. The degree of hydration from hydrations performed in acetic acid can possibly also be explained by the hydrolysis reaction of the acetate ions.

The low degree of hydration in sodium acetate is caused by the high pH of the solution as shown in Figure 4.7 (this will be dealt with in detail in Section 4.5), and the low concentration of Mg^{2+} ions.

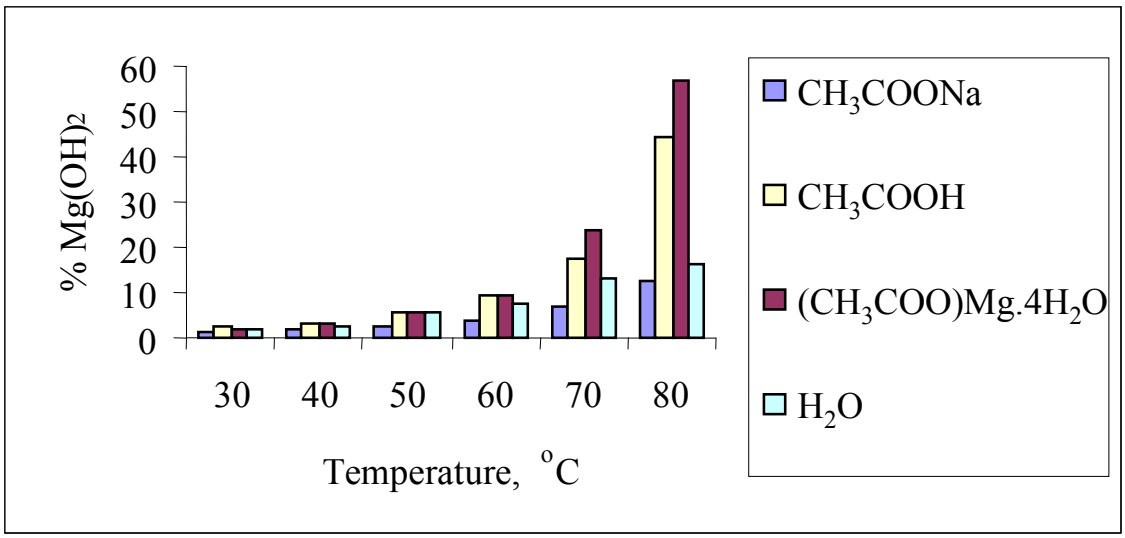

Figure 4.4. Effect of CH_3COONa, CH_3COOH, $(CH_3COO)Mg.4H_2O$ and H_2O on the degree of hydration

Magnesium chloride, hydrochloric acid, ammonium chloride and water are compared in Figure 4.5. The figure shows that all hydrating agents produced less than 10 % of magnesium hydroxide up to 50 ^oC. At 60 ^oC, hydrochloric acid formed more magnesium hydroxide in comparison to magnesium chloride and ammonium chloride. At 70 ^oC, magnesium chloride and hydrochloric acid performed better than ammonium chloride. At 80 ^oC, ammonium chloride performed better than hydrochloric acid and magnesium chloride. Water was again the ineffective hydrating agent when compared to the other hydrating agents.

The increase in the degree of hydration in the NH_4Cl solutions can also be explained by a hydrolysis reaction. After ionization of NH_4Cl, the NH_4^+ ion may also undergo hydrolysis:

$$NH_4^+(aq) + H_2O(\ell) \rightarrow NH_3(aq) + H_3O^+(aq)$$

The H_3O^+ formed from the hydrolysis of NH_4^+ can then increase the dissolution of MgO to form more Mg^{2+}. This can possibly explain why NH_4Cl behaves approximately the same as HCl and HNO_3.

The enhanced degree of hydration from hydration performed in magnesium chloride when compared to water is possibly due to the additional Mg^{2+} ions in the magnesium chloride solution.

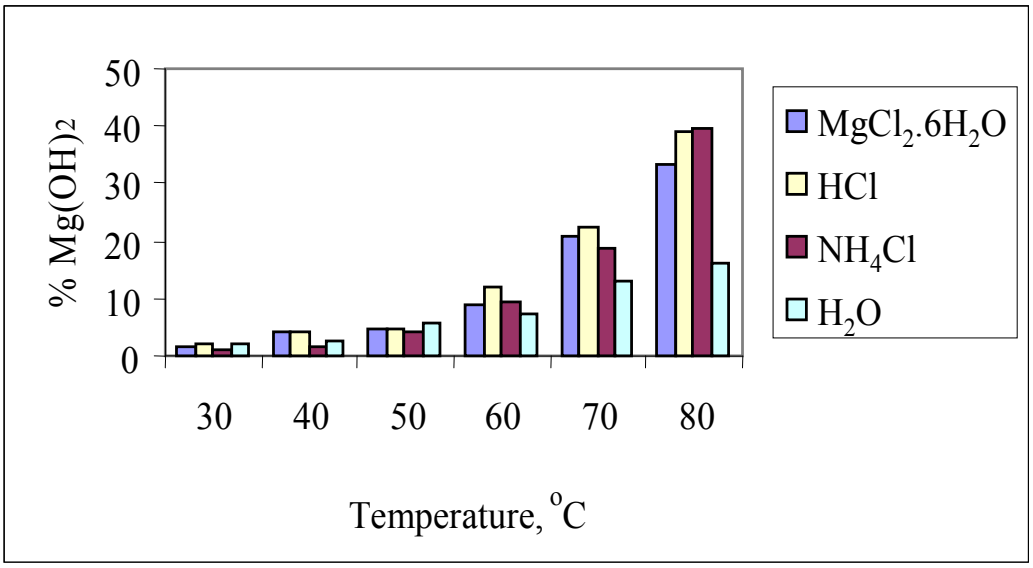

Figure 4.5. Effect of $MgCl_2.6H_2O$, HCl, NH_4Cl and H_2O on the degree of hydration

The magnesium containing hydrating agents and water are compared in Figure 4.6. The figure shows that there was not a significant difference in the hydration behaviour of the hydrating agents up to 50 ^oC. At 60 ^oC, magnesium nitrate seemed to be a good hydrating agent while magnesium chloride and magnesium acetate gave similar results. Magnesium chloride and magnesium acetate gave similar results at 70 ^oC while magnesium acetate produced a larger percentage of magnesium hydroxide. At 80 ^oC, magnesium acetate formed the largest percentage of magnesium hydroxide when compared to the other hydrating agents. When compared to the hydrations in magnesium chloride and magnesium nitrate, the increased degree of hydration in magnesium acetate seemed to be due to the higher concentration of Mg^{2+} ions in the solution. At 80 ^oC, the hydration performed in magnesium nitrate resulted in a larger percentage of magnesium hydroxide being produced than in the case of magnesium chloride.

The increased degree of hydration in magnesium acetate is due to the presence of acetate ions as described in the introduction (Section 1.4.1) and the additional Mg^{2+} ions. When compared to the hydration in water, all the hydrating agents, with the exception of sodium acetate, seemed to be effective hydrating agents. The complexation power of the anions (e.g. acetate ions) with Mg^{2+} ions during MgO

dissolution affects the reaction rate (Filippou et al., 2004). It seems that hydration reactions are dependent upon the MgO solubility in the hydrating agent solutions.

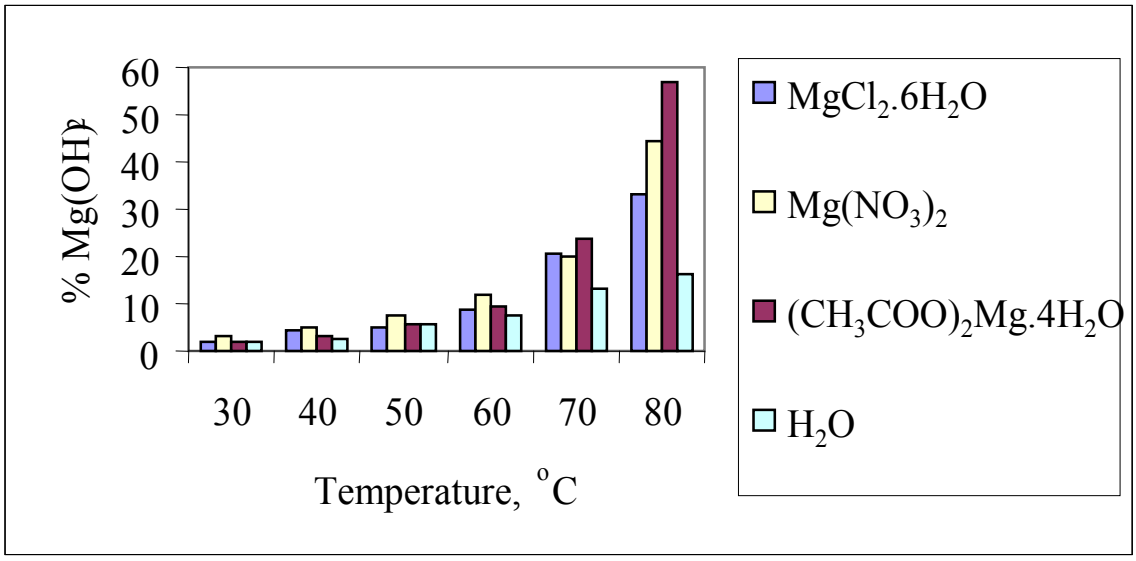

Figure 4.6. Effect of $MgCl_2.6H_2O$, $Mg(NO_3)_2$, $(CH_3COO)_2Mg.4H_2O$ and H_2O on the degree of hydration

4.5 Variation of pH with hydration temperature and hydrating agents

Figures B1-B9 (Appendix) depict the variations of the hydration solution pH with temperature for the hydration of magnesium oxide in different hydrating agents. For all hydrating agents, a decrease in solution pH was observed when the hydration temperature was increased. The variation of pH during the progress of reaction observed in a number of experiments, exclusive of water and sodium acetate, indicated a low pH at the start, thereafter an increase in pH and finally a drop in pH due to the solubility of magnesium hydroxide in aqueous solution. For hydrations in water and sodium acetate, an increase in pH with time was observed. The increase in pH from the hydration performed in water at the 25th minute resulted after the stirrer was stopped to allow for the solids to settle. The difference in the solutions' pH values is possibly due to the solubilities of magnesium oxide in different hydrating agents as a function of temperature.

The pH-time graphs indicated an increase in the pH values during the first five minutes of the hydration reaction. This may indicate that the rate of formation of magnesium hydroxide is high in the first few minutes of hydration. Rocha et al (2004) suggested that the magnesium hydroxide solubility reduces as the temperature of the system is raised. These authors indicated that supersaturation is reached rapidly in a few minutes. At lower temperatures, agglomerates of magnesium hydroxide are generated leading to higher pH values and Mg^{2+} concentrations. A slight drop in the pH curve may be attributed to the precipitation of magnesium hydroxide causing the aqueous solution to be more acidic.

As can be seen from the graphs, the hydration reaction takes place at pH values ranging between 7 and 11.5. Fruhwirth et al (1985) pointed out that at pH values below 11.5, the rate-determining step was OH^- adsorption followed by Mg^{2+} and OH^- desorption leading to a rate maximum. The reaction below describes the overall dissolution process at pH values below 11.5:

$$MgOH^+(surface) + OH^- \rightarrow MgOH^+.OH^-(surface) \rightarrow Mg^{2+}(aq) + 2\,OH^-(solution)$$

Fruhwirth et al (1985) suggested that the OH^- ions' adsorption followed by the Mg^{2+} ions' desorption are critical steps in dissolving magnesium hydroxide in solution at pH values below 11.5.

Figure 4.7 depicts the variation of the average pH, obtained between 20 and 30 minutes of hydration, with the hydration temperature for the different hydrating agents. The trend in the variation is similar for all the hydrating agents, i.e., the pH decreases as the temperature increases. The figure shows that all the hydration experiments took place at pH values ranging between 7 and 11. Higher pH values were observed for the hydration reactions performed in sodium acetate and water, when compared to the hydration reactions performed in the other hydrating agents. The hydration reactions performed in sodium acetate resulted in even higher pH values compared to those performed in water. The other hydrating agents (hydrochloric acid, acetic acid, nitric acid, magnesium nitrate, magnesium chloride, ammonium chloride and magnesium acetate) had approximately similar pH values.

The figure shows that at lower temperatures, the pH values are higher possibly due to an increase in the solubility of magnesium hydroxide in the solution. This resulted in a lower amount of magnesium hydroxide being formed. The magnesium hydroxide solubility decreases as the temperature is raised while an increase in temperature increases the solubility of magnesium oxide (Rocha et al., 2004). The precipitation of magnesium hydroxide is increased at higher temperatures, causing the aqueous solution to be more acidic and therefore the pH to be lower. Fruhwirth et al (1985) indicated that the dissolution rate of MgO can be measured by a change in pH. A decrease in pH resulted in a high dissolution rate whereas a low dissolution rate can be attributed to a high pH. The lower degree of hydration in sodium acetate is possibly caused by the high pH values as indicated in Fig 4.7, and the lower amount of OH^- ions produced. Literature indicates that the degree of hydration greatly decreases in strong basic region due to a lower MgO solubility (Fruhwirth, et al., 1985), and this further supports observations made in this study (see Fig. 4.7).

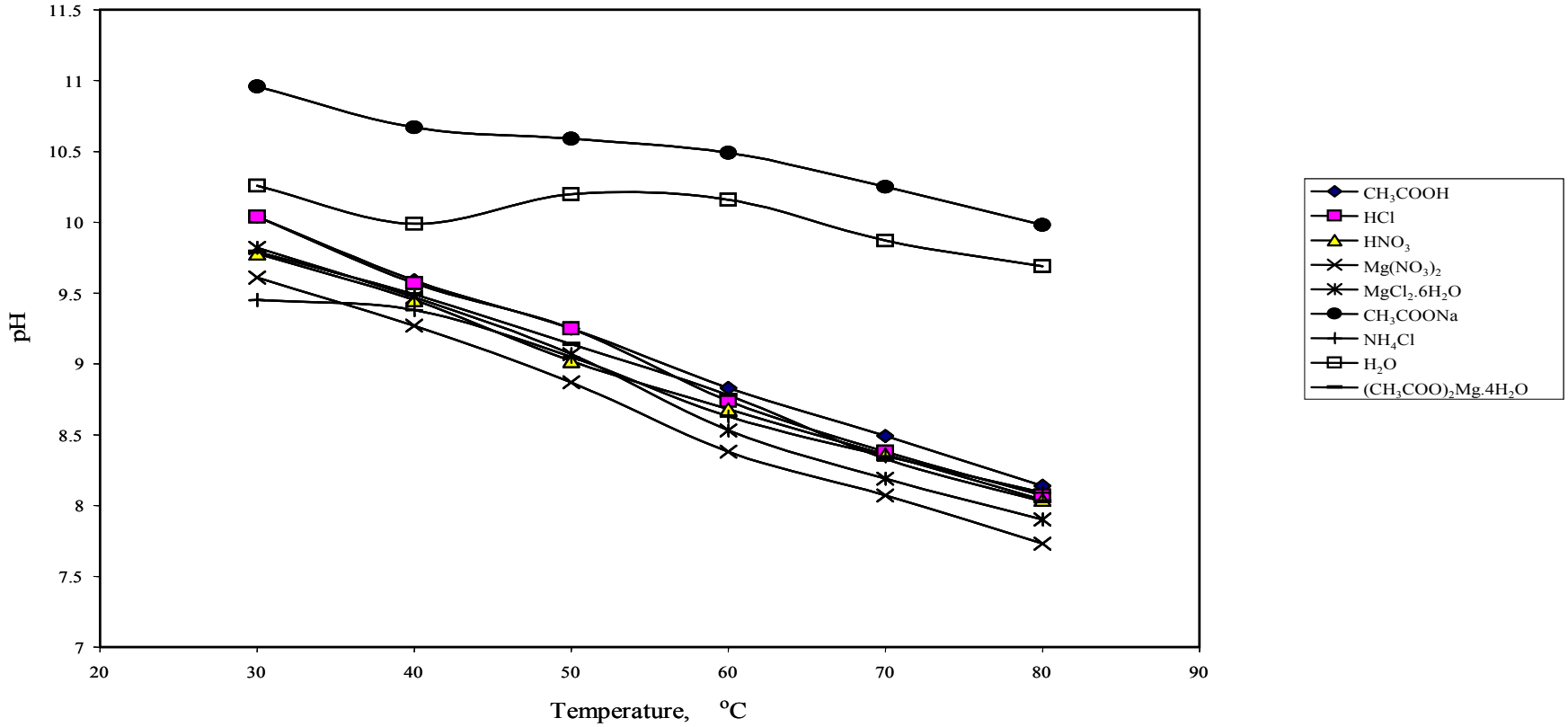

Figure 4.7 Variation of the average pH with hydration temperature for the different hydrating agents.

4.6 XRD of products hydrated at 80 ^{o}C

Tables 4.5, 4.6 and Figures A3-A11 (Appendix) show the quantitative analysis and XRD spectra of the products obtained after hydration at 80 ^{o}C. It clearly shows that the phases present after hydration were mainly $Mg(OH)_2$ and unreacted MgO, while small amounts of magnesite and quartz could also be observed. The hydrations performed in magnesium acetate, magnesium nitrate and acetic acid resulted in an optimum amount of $Mg(OH)_2$ being formed when compared to the other hydrating agents. The major phase constituent in the products obtained from hydrations in ammonium chloride, water, magnesium chloride, sodium acetate and hydrochloric acid appeared to be MgO.

Table 4.7 shows a comparison of the degree of hydration as determined by TGA and XRD after hydration at 80 ^{o}C. The XRD results of the hydrations performed in magnesium acetate, water and sodium acetate compare very well with their thermogravimetric results. The percentages of magnesium hydroxide in ammonium chloride, magnesium nitrate, nitric acid, acetic acid, magnesium chloride and hydrochloric acid are not the same as the quantitative XRD results. The difference in these results can be ascribed to the difference in sample analysis time of the two techniques. Thermogravimetric analyses were performed immediately after drying the sample at 200 ^{o}C while XRD samples were not done immediately after preparation. It seems that the XRD analyses were done on samples that absorbed moisture.

Table 4.5. XRD analysis of products hydrated in NH_4Cl, $Mg(CH_3COO)_2.4H_2O$, $Mg(NO_3)_2$ and $HN0_3$ at 80 ^oC

	NH_4Cl	$Mg(CH_3COO)_2.4H_2O$	$Mg(NO_3)_2$	$HN0_3$
$Mg(OH)_2$	43.45±1.62%	58.34±1.53%	51.30±1.38%	47.18±1.53%
$MgCO_3$	0.81±0.63%	0.28±0.39%	0.45±0.45%	0.53±0.48%
MgO	55.43±1.62%	41.09±1.50%	47.85±1.38%	51.88±1.53%
SiO_2	0.31±0.18%	0.29±0.18%	0.40±1.23%	0.40±0.24%

Table 4.6. XRD analysis of products hydrated in CH_3COOH, H_2O, $MgCl_2.6H_2O$, $NaCH_3COO$ and HCl at 80 ^oC

	CH_3COOH	H_2O	$MgCl_2.6H_2O$	$NaCH_3COO$	HCl
$Mg(OH)_2$	54.72±0.51%	15.61±1.56%	45.07±0.39%	13.70±1.59%	47.79±0.39%
$MgCO_3$	0.29±0.24%	0.00±0.00%	0.00±0.00%	0.91±0.75%	0.00±0.00%
MgO	44.60±0.51%	84.00±1.56%	54.42±0.36%	84.89±1.68%	51.70±0.39%
SiO_2	0.39±0.15%	0.39±0.17%	0.51±0.16%	0.50±0.21%	0.51±0.16%

Table 4.7. A comparison between the degree of hydration as determined by TGA and XRD after hydration at 80 ^{o}C

	NH_4Cl	$Mg(CH_3COO)_2.4H_2O$	$Mg(NO_3)_2$	$HN0_3$	CH_3COOH	H_2O	$MgCl_2.6H_2O$	$NaCH_3COO$	HCl
% $Mg(OH)_2$ by TGA	39.7	56.7	44.4	38.8	44.5	16.1	33.1	12.2	39.1
% $Mg(OH)_2$ by XRD	43.45	58.34	51.30	47.18	54.72	15.61	45.07	13.70	47.79

4.7 Surface area

The calcined magnesite gave a surface area of 73.48 m^2/g with a citric acid reactivity of 14 seconds, which indicates a highly reactive magnesium oxide. After calcination at 1200 ^oC for 1 hour, the measured surface area was 5.04 m^2/g and the citric acid reactivity values ranged between 510 and 590 seconds.

Figure 4.8 summarizes the specific surface areas of the products after 30 minutes of hydration within the temperature range of 30-80 ^oC. The surface areas of the products, exclusive of products obtained from hydrations performed in magnesium acetate and acetic acid, decreased slightly at a hydration temperature of 80 ^oC. Magnesium acetate and acetic acid showed an increase in product surface areas with increasing temperature. The products formed from hydration in water had surface areas close to those obtained from hydration in ammonium chloride, magnesiun nitrate, nitric acid, hydrochloric acid, sodium acetate and magnesium chloride

Surface areas of 9.10 m^2/g at 60 ^oC to 16.07 m^2/g at 80 ^oC were obtained from the hydration in acetic acid. Upon hydration in magnesium acetate, surface areas of 10.47 m^2/g at 60 ^oC and 28.44 m^2/g at 80 ^oC were obtained. Magnesium acetate was the hydrating agent that showed the strongest temperature dependence, with the highest product surface areas.

According to Fillipou et al (2004), very rapid hydration of magnesium oxide will result in the formation of relatively big hydroxide aggregates consisting of submicroscopic crystallites with very high surface area-particle morphology. This can explain the higher surface areas of products formed from the hydration in magnesium acetate and acetic acid. It seemed that the products were formed at a rate that decreased the possibility of crystal formation and that smaller magnesium hydroxide particles, resulting in higher surface areas, were formed (Van der Merwe, et al., 2006).

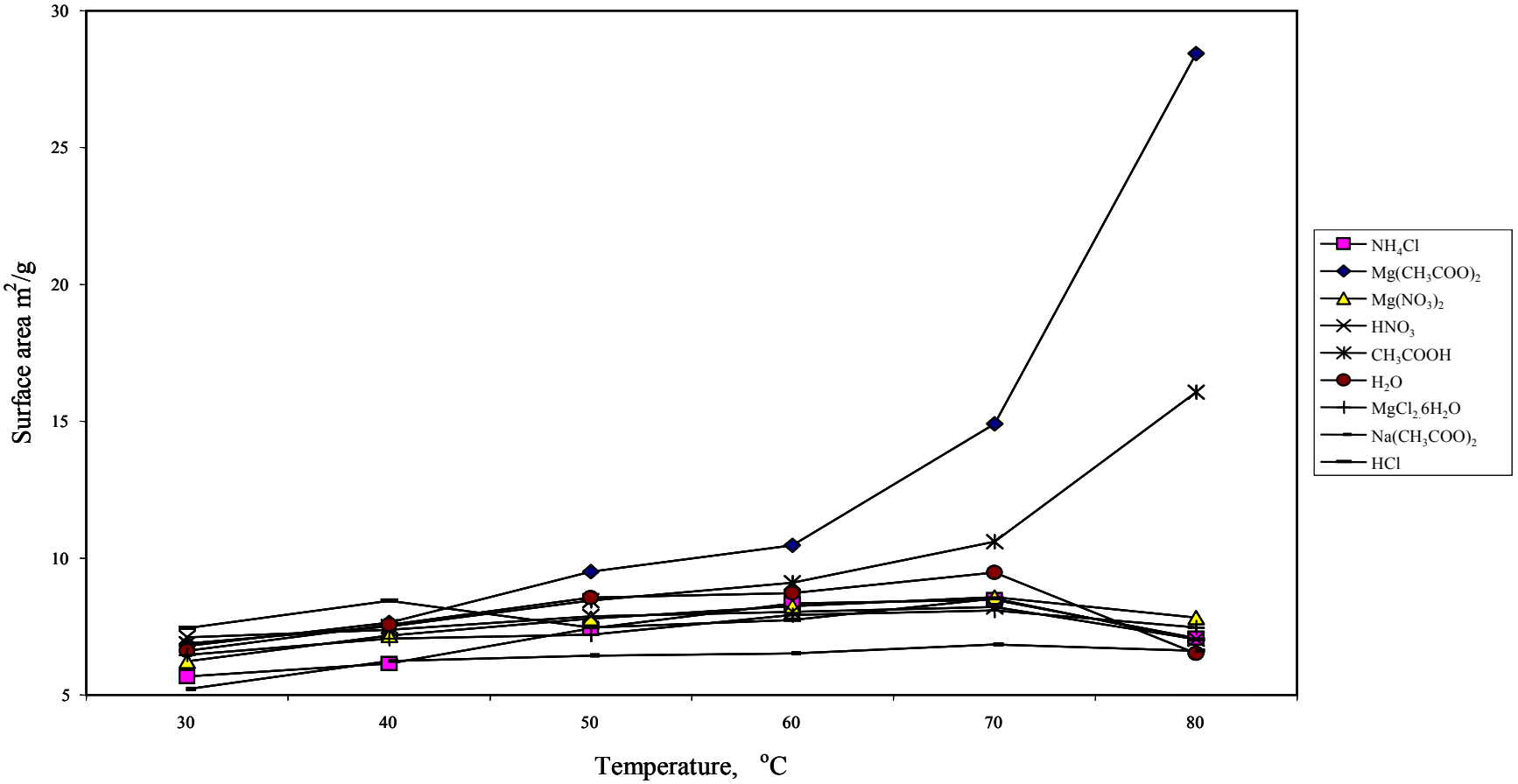

Figure 4.8 The variation of product surface area with hydration temperature

CHAPTER 5

CONCLUSIONS

The effects of hydrating solutions on the hydration of magnesium oxide were investigated. The results indicated that the degree of hydration is very sensitive to the hydration temperature. The optimum amount of magnesium hydroxide formed at higher temperatures is due to the better solubility of magnesium oxide at these temperatures and therefore the precipitation of magnesium hydroxide is high. At lower temperatures, the solubility of magnesium oxide is low, while that of magnesium hydroxide is increased (Rocha, et al., 2004). This resulted in a decrease in the amount of magnesium hydroxide formed at lower temperatures.

When compared to the hydration in water, all the hydrating agents applied in this study, with the exception of sodium acetate, seemed to increase the degree of hydration of MgO. The low degree of hydration for the hydrations performed in sodium acetate is probably due to the higher pH of the hydration solution, and the lower concentration of Mg^{2+} ions in the solution. Fruhwirth et al (1985) indicated that the degree of hydration is significantly reduced at higher pH values, due to a decrease in the MgO solubility.

The degree of hydration from the hydrations performed in magnesium acetate, magnesium nitrate and acetic acid improved significantly at 80 ^{o}C when compared to the other hydrating agents. The highest amount of magnesium hydroxide was obtained for the hydration performed in magnesium acetate. There was not a significant difference in the hydration behavior of the hydrating agents up to 50 ^{o}C, where less than 10 % of magnesium hydroxide was formed.

Botha et al (2001) reported that the chemical process through which magnesium acetate enhances the degree hydration can be ascribed to differences in the solubility of the various magnesium compounds in the slurry. Filippou et al (2004) reported that the high yield of magnesium hydroxide from hydrations performed in magnesium

acetate can be attributed to the presence of acetate ions. The reaction mechanism proposed by Filippou et al entails the dissociation of magnesium acetate into acetate and magnesium ions, after which the magnesia particles dissolve to give a magnesium-acetate complex ion. After that, the dissociation of the magnesium-acetate complex ion into acetate and magnesium ions takes place, followed by magnesium hydroxide precipitation in the bulk of the solution due to supersaturation. This mechanism provides a possible explanation for the enhanced degree of hydration in magnesium acetate and acetic acid solutions. The difference in performance between acetic acid and magnesium acetate as hydrating agents can be ascribed to the additional Mg^{2+} ions, which will further increase the degree of hydration in magnesium acetate.

It seems that the reaction mechanism that explains the hydration of MgO in magnesium acetate best comprises the ionization of magnesium acetate into magnesium and acetate ions. Thereafter, hydrolysis of the acetate ion takes place to produce acetic acid and hydroxyl ions. Magnesium hydroxide is then formed from the reaction between the Mg^{2+} and OH^- ions. The acetic acid can then react with MgO to form magnesium acetate, and the above series take place, over and over, each cycle leading to more magnesium hydroxide being formed.

The enhanced degree of hydration for the hydrations performed in acidic hydrating agents seems to be due to the higher concentration of H^+ ions in the solution, by increasing the solubility of magnesium oxide through the following reaction:

$$MgO\ (s) + 2\ H^+\ (aq) \rightarrow Mg^{2+}\ (aq) + H_2O\ (l)$$

It seems that the hydration reactions are dependent upon the magnesium oxide solubility in the hydrating agent solutions. Jost et al (1997) explained the higher degree of hydration of magnesium oxide in magnesium chloride by an increase in the solubility of magnesium oxide in magnesium chloride solutions.

It was clear that the pH of the solution plays a crucial role during hydration. Differences in the hydrating solutions' pH could be attributed to differences in the solubility of MgO in different hydrating agents as a function of temperature. In general, a decrease in solution pH was observed with an increase in solution

temperature. The degree of hydration decreased at higher pH values due to the low H^+ and low Mg^{2+} ions concentration, while the highest amount of magnesium hydroxide was obtained at lower pH values. All the hydration reactions took place at pH values ranging between 7 and 11.5.

XRD analyses confirmed that the products obtained consisted mainly of magnesium hydroxide, unreacted magnesium oxide and small amounts of magnesite and quartz. The amount of magnesium hydroxide formed varied for each hydrating agent used.

The surface areas of most of the products were in the range of 5 – 10 m^2/g. However, magnesium acetate and acetic acid showed a significant increase in product surface area with increasing temperature. The surface area increased from 5.04 m^2/g for the calcined magnesite before hydration to 28.44 m^2/g for the product after hydration in magnesium acetate at 80 °C. Fillipou et al (2004) reported that very rapid hydration of magnesia will result in the formation of relatively big hydroxide aggregates consisting of submicroscopic crystallites with very high surface area-particle morphology. From the surface area results, it was clear that the variation of product surface area with temperature had stronger temperature dependence for the hydrations performed in magnesium acetate and acetic acid, compared to the other hydrating agents applied in this study. It seems that the hydration of magnesium oxide takes places via a different mechanism in the presence of acetate ions.

This study has shown that hydrating solutions, other than water, can successfully be applied to increase the degree of hydration of magnesium oxide to magnesium hydroxide.

APPENDIX (XRD SPECTRA)

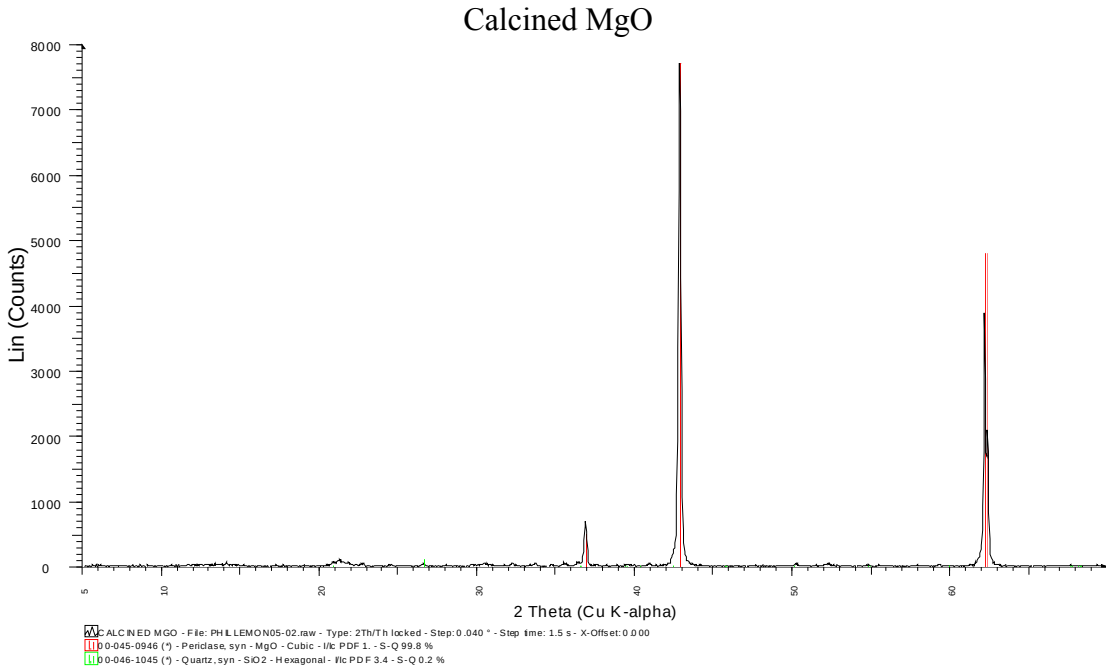

Figure A1. XRD pattern of calcined MgO

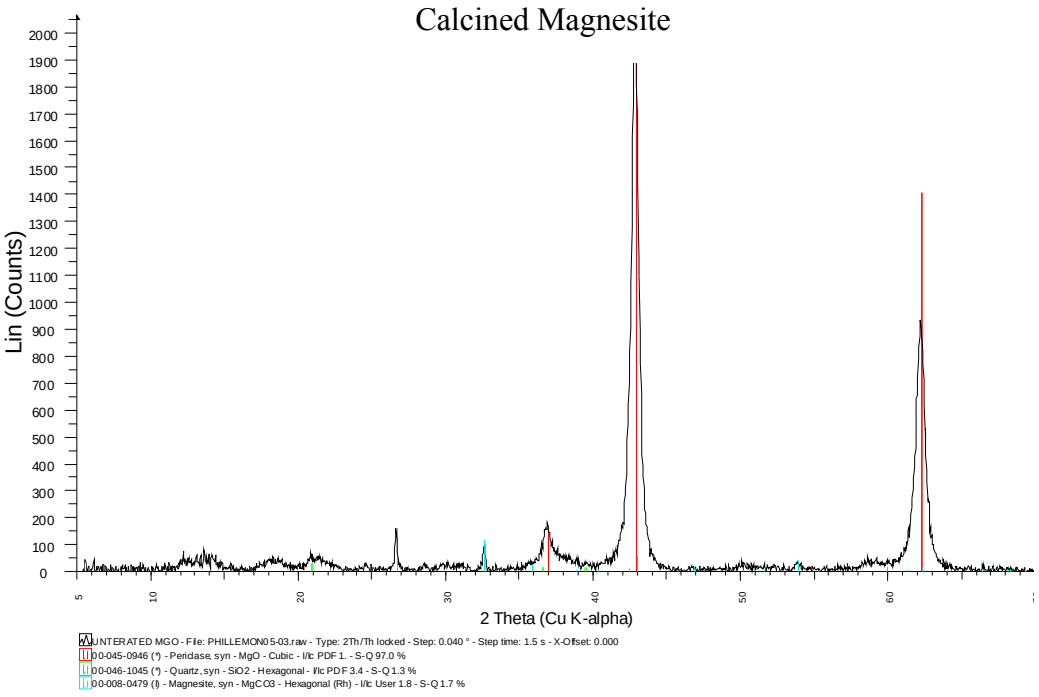

Figure A2. XRD pattern of the calcined magnesite

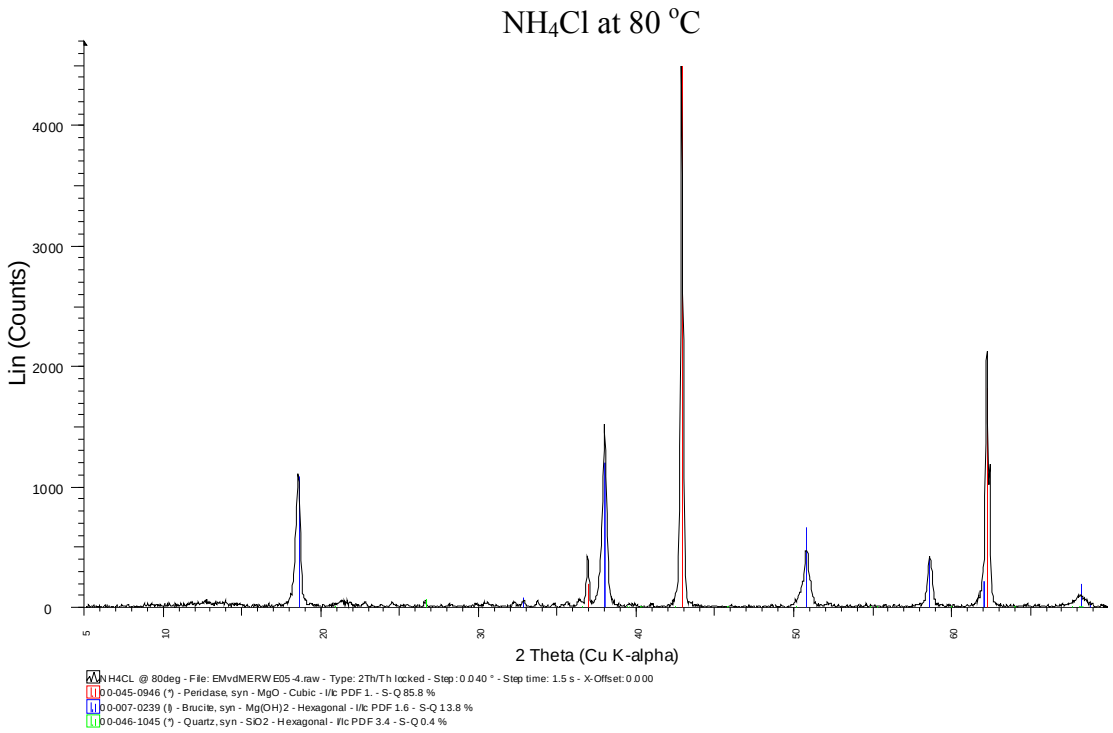

Figure A3. XRD pattern of product obtained from hydration in ammonium chloride

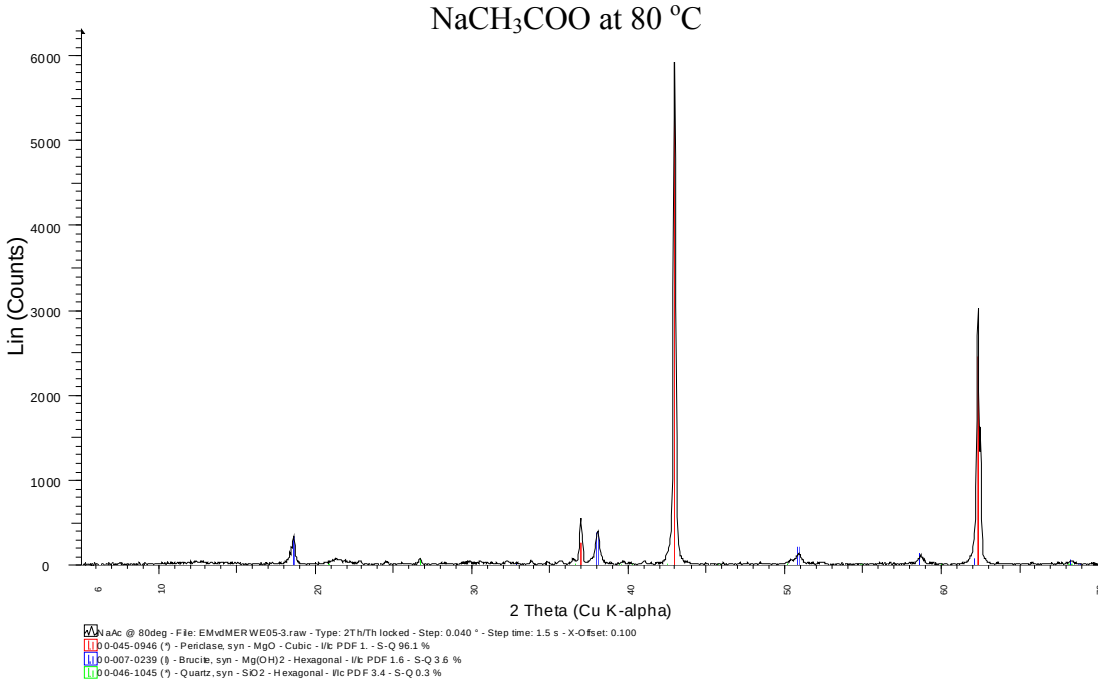

Figure A4. XRD pattern of product obtained from hydration in sodium acetate

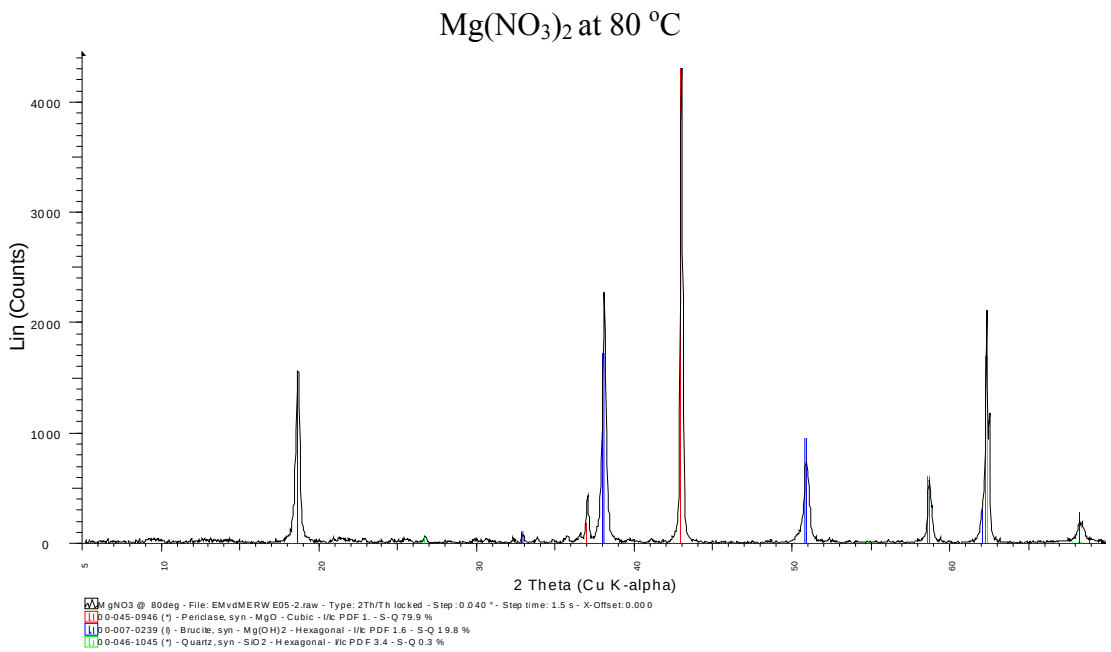

Figure A5. XRD pattern of product obtained from hydration in magnesium nitrate

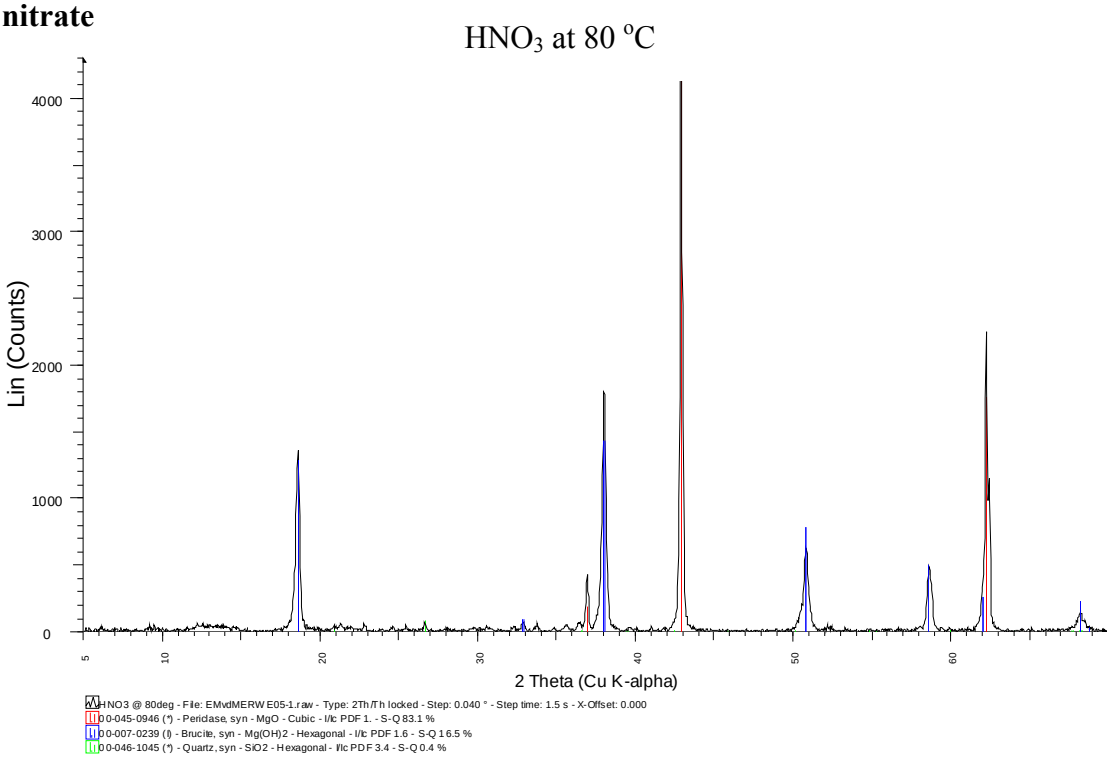

Figure A6. XRD pattern of product obtained from hydration in nitric acid

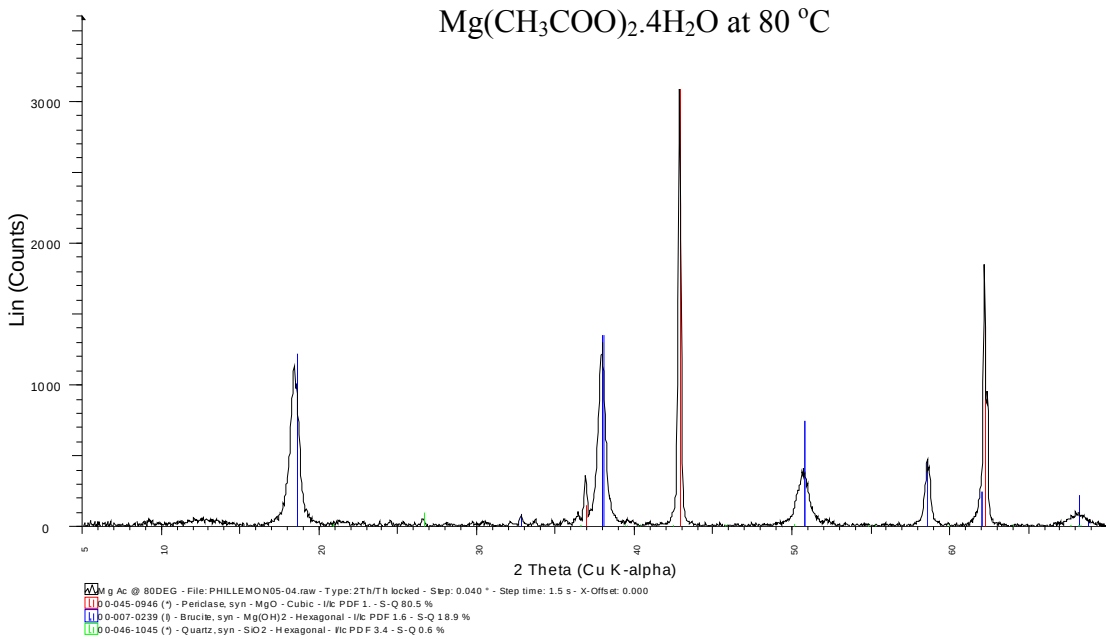

Figure A7. XRD pattern of product obtained from hydration in magnesium acetate

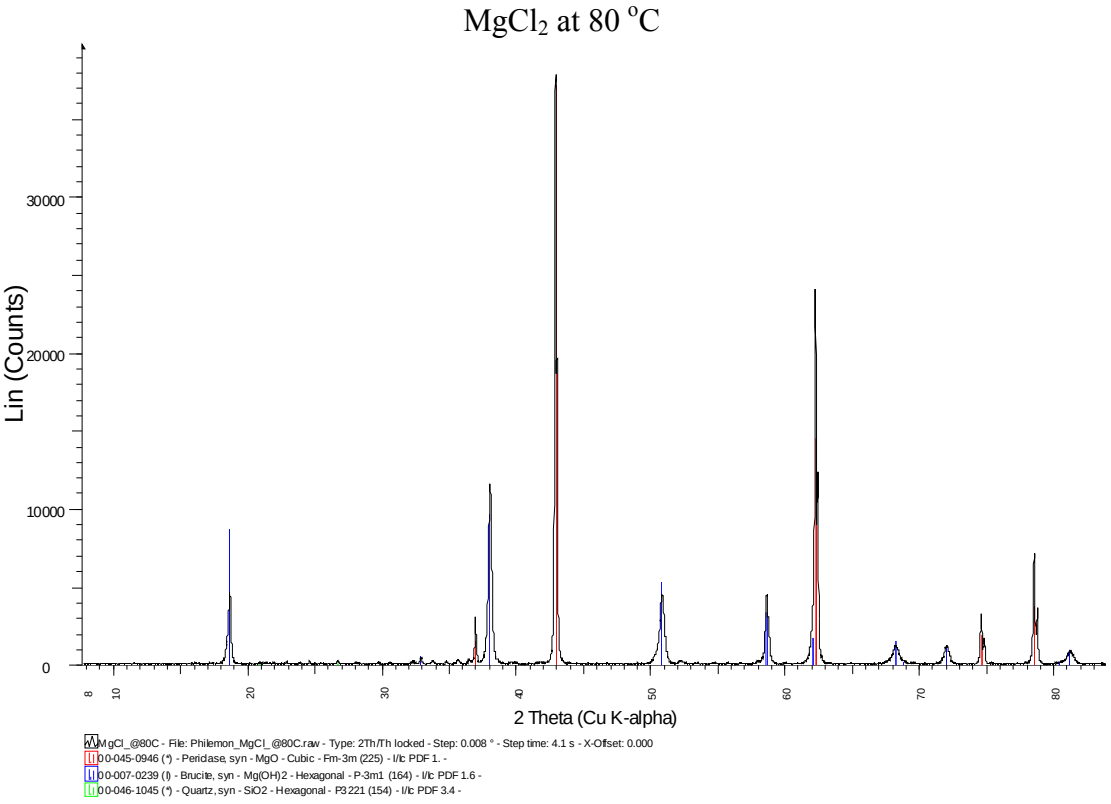

Figure A8. XRD pattern of product obtained from hydration in magnesium chloride

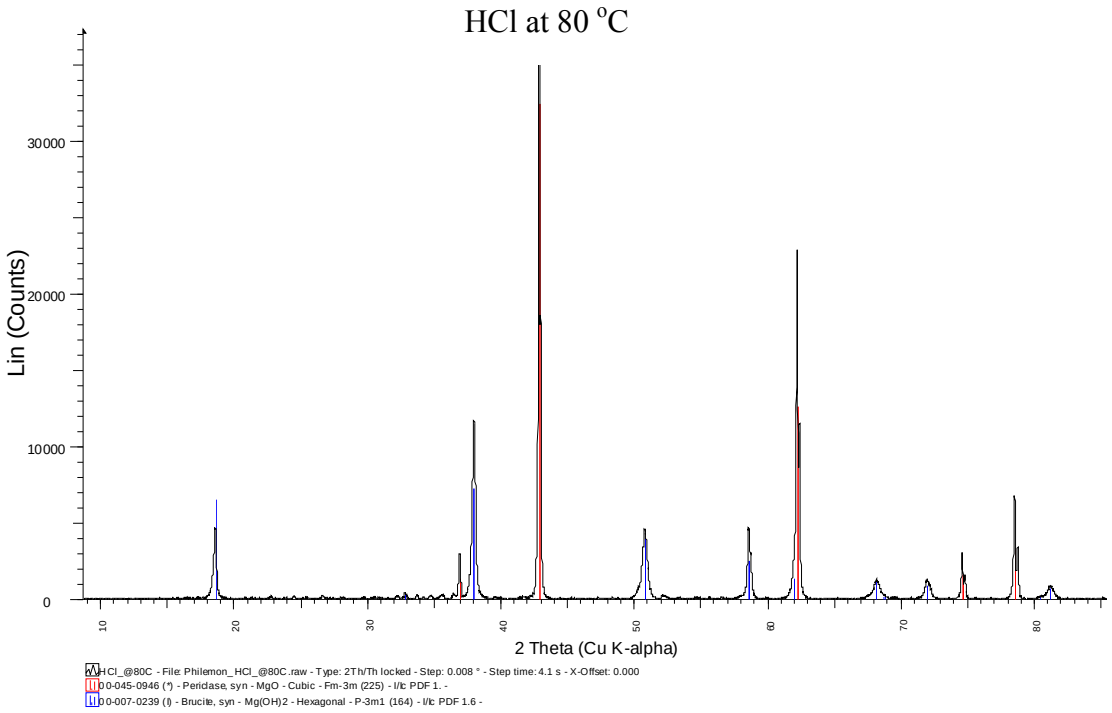

Figure A9. XRD pattern of product obtained from hydration in hydrochloric acid

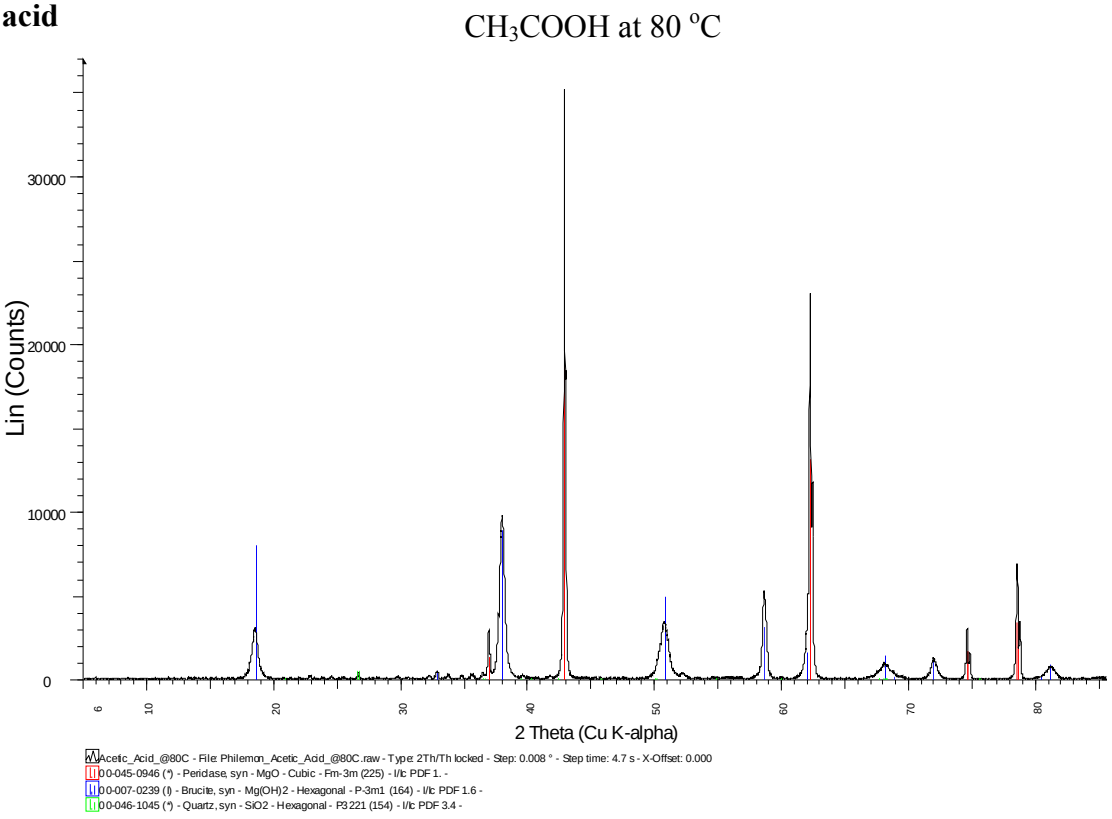

Figure A10. XRD pattern of product obtained from hydration in Acetic acid

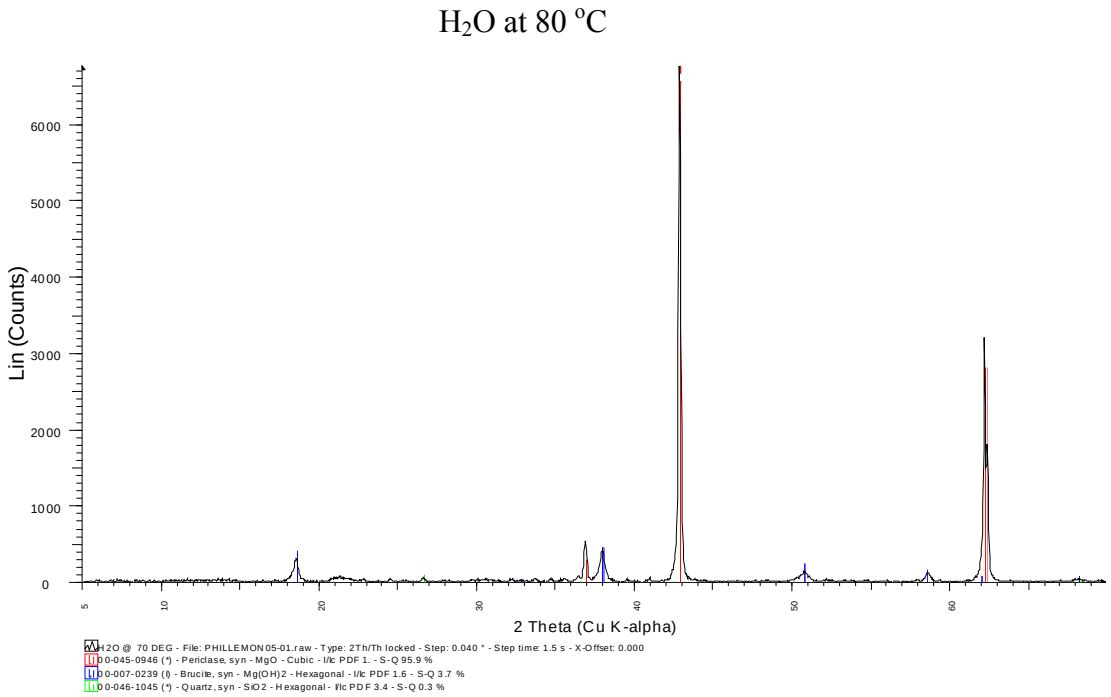

Figure A11. XRD pattern of product obtained from hydration in water

APPENDIX (pH-TIME GRAPHS)

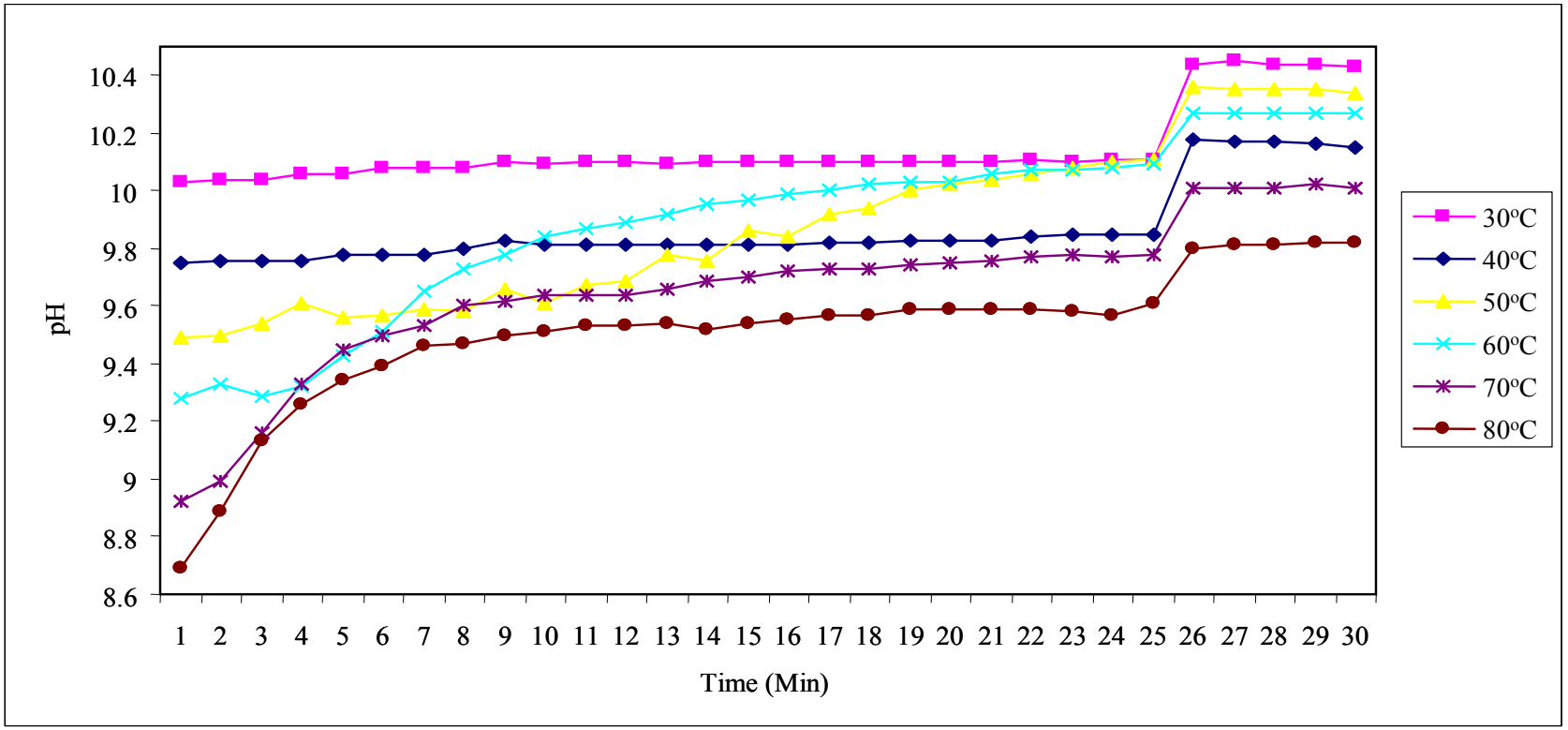

Figure B1. Variation of pH with temperature for the hydration of MgO in water

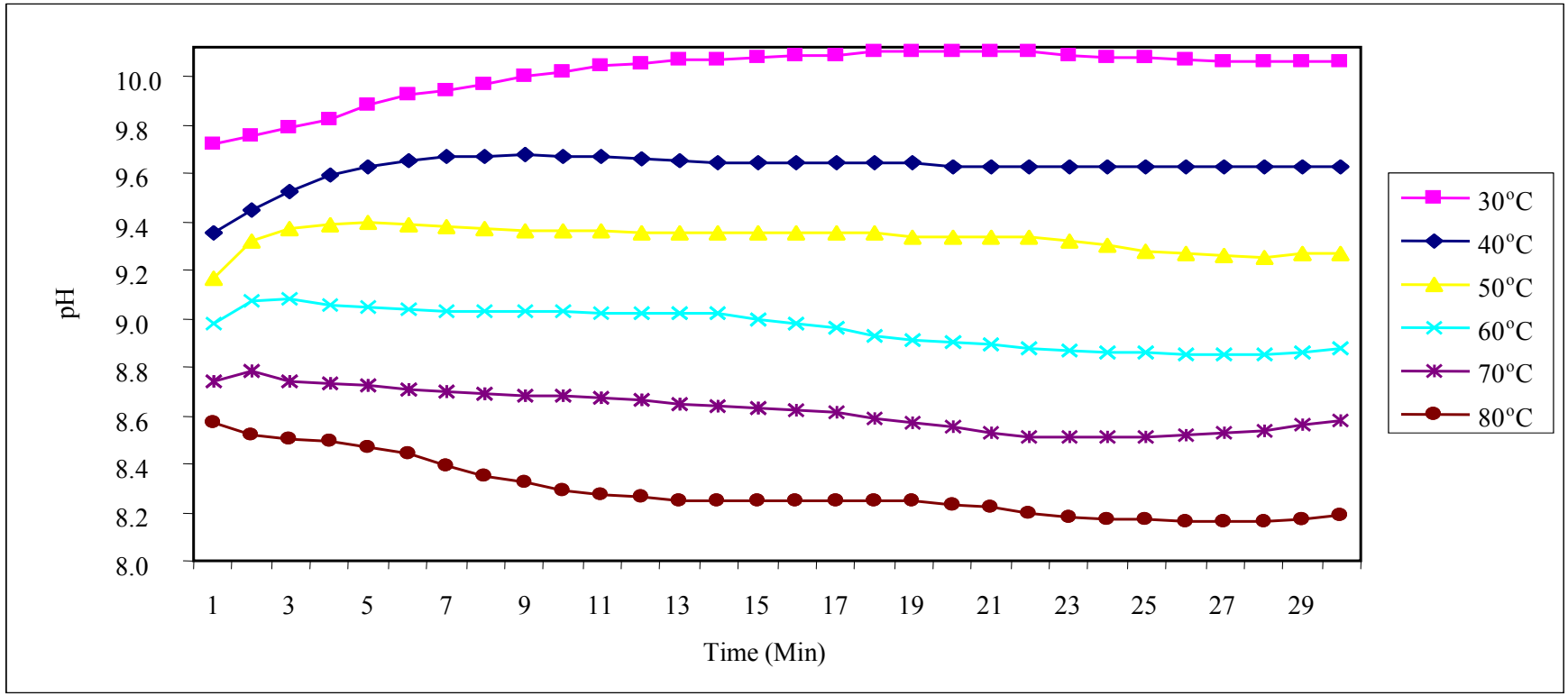

Figure B2. Variation of pH with temperature for the hydration of MgO in acetic acid

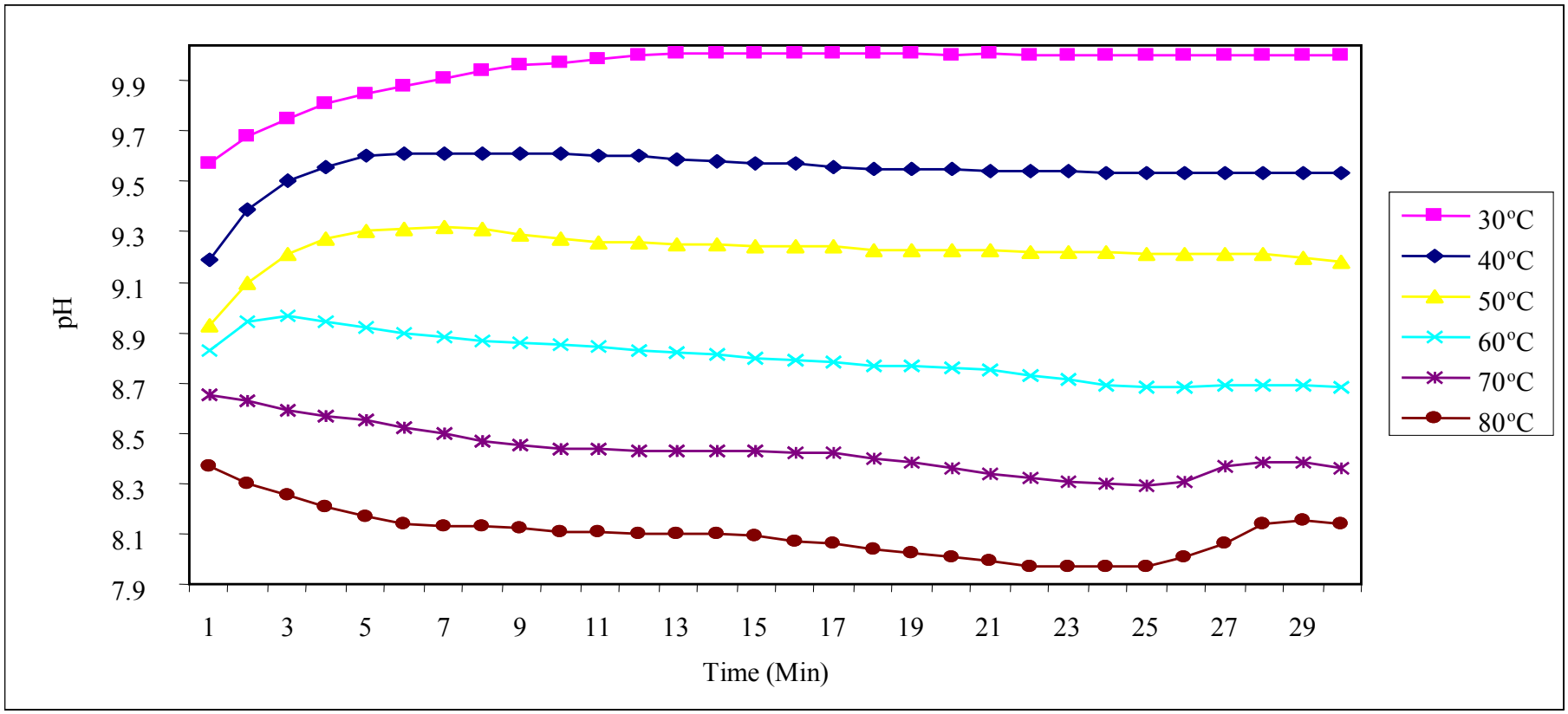

Figure B3. Variation of pH with temperature for the hydration of MgO in hydrochloric acid

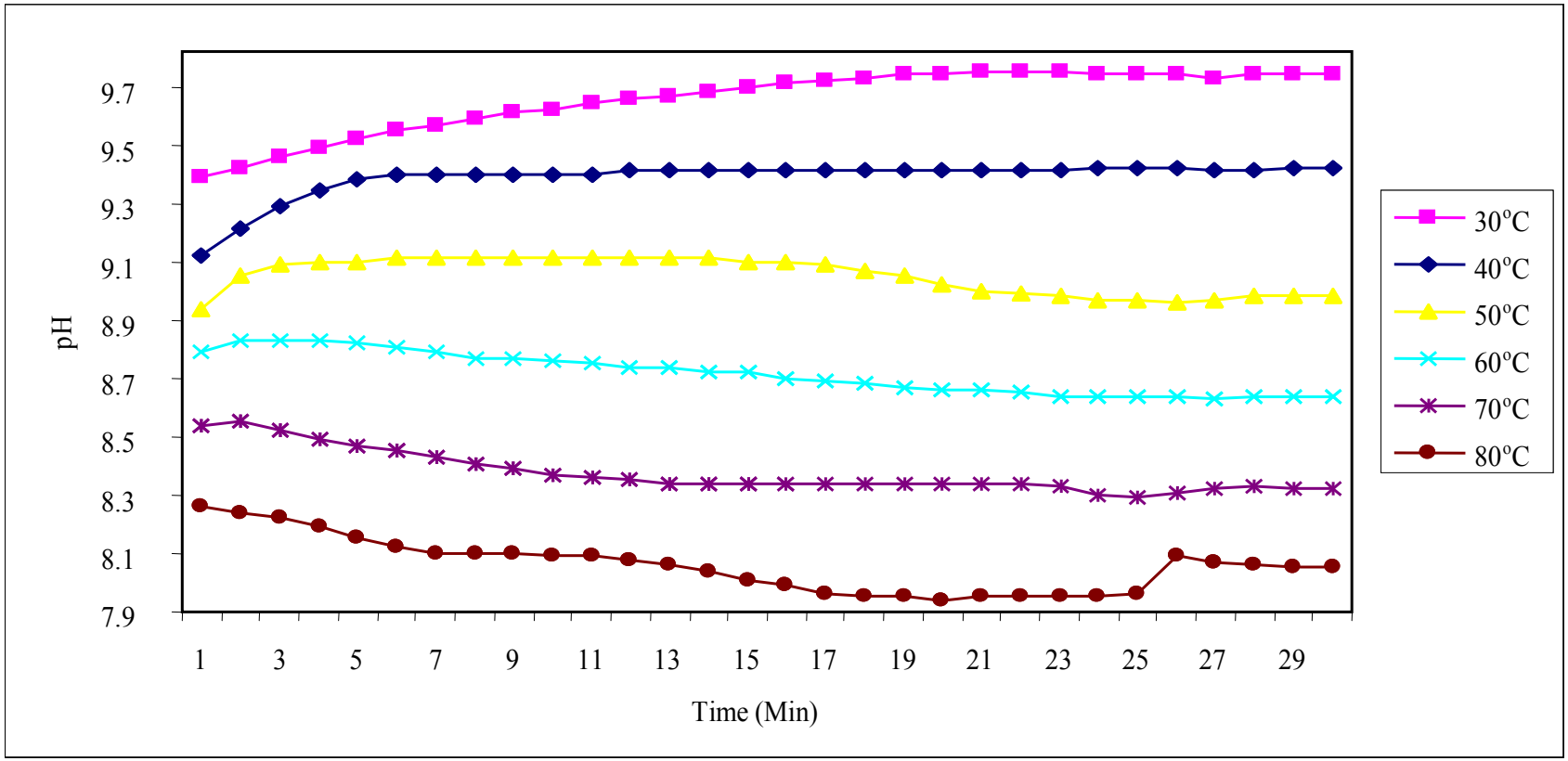

Figure B4. Variation of pH with temperature for the hydration of MgO in nitric acid

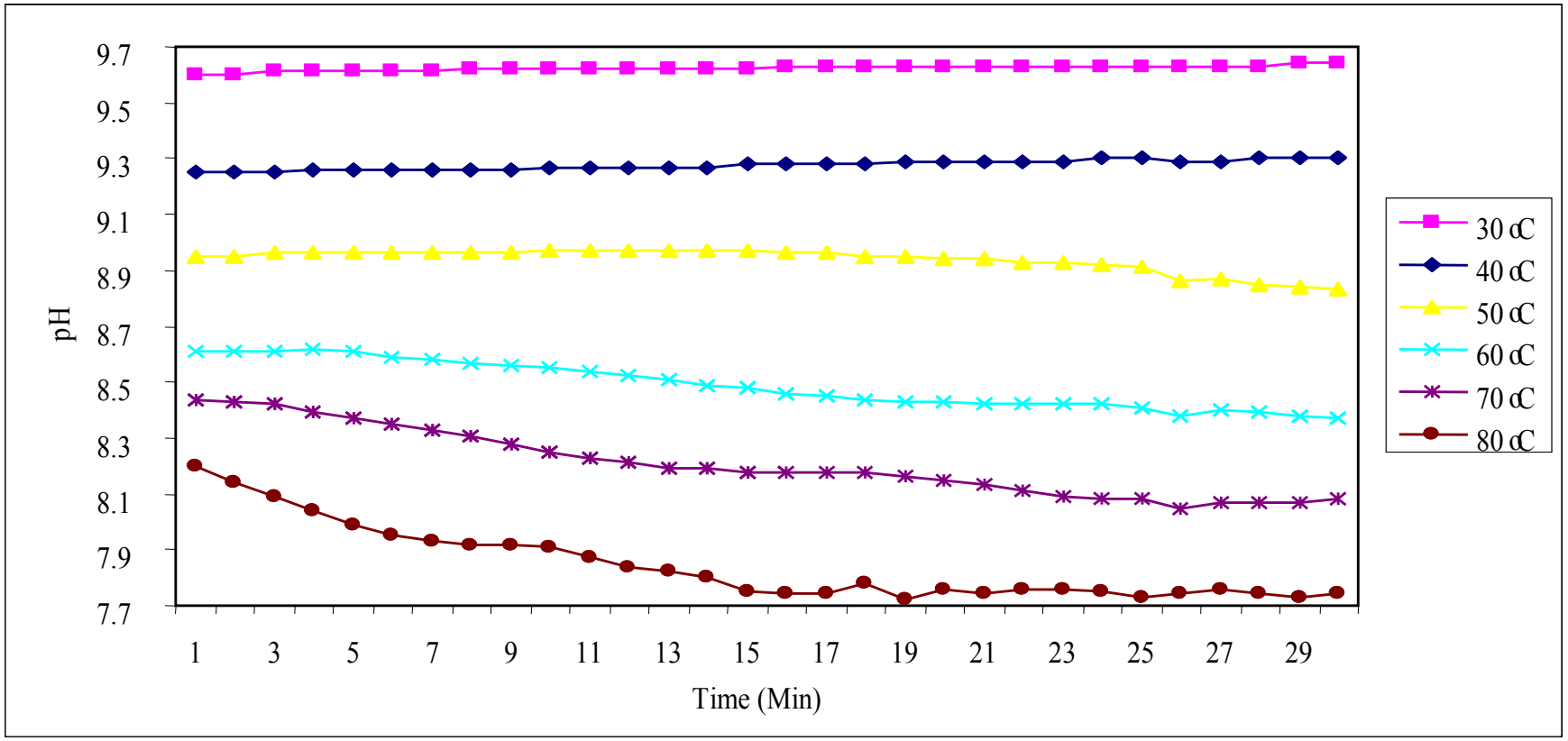

Figure B5. Variation of pH with temperature for the hydration of MgO in magnesium nitrate

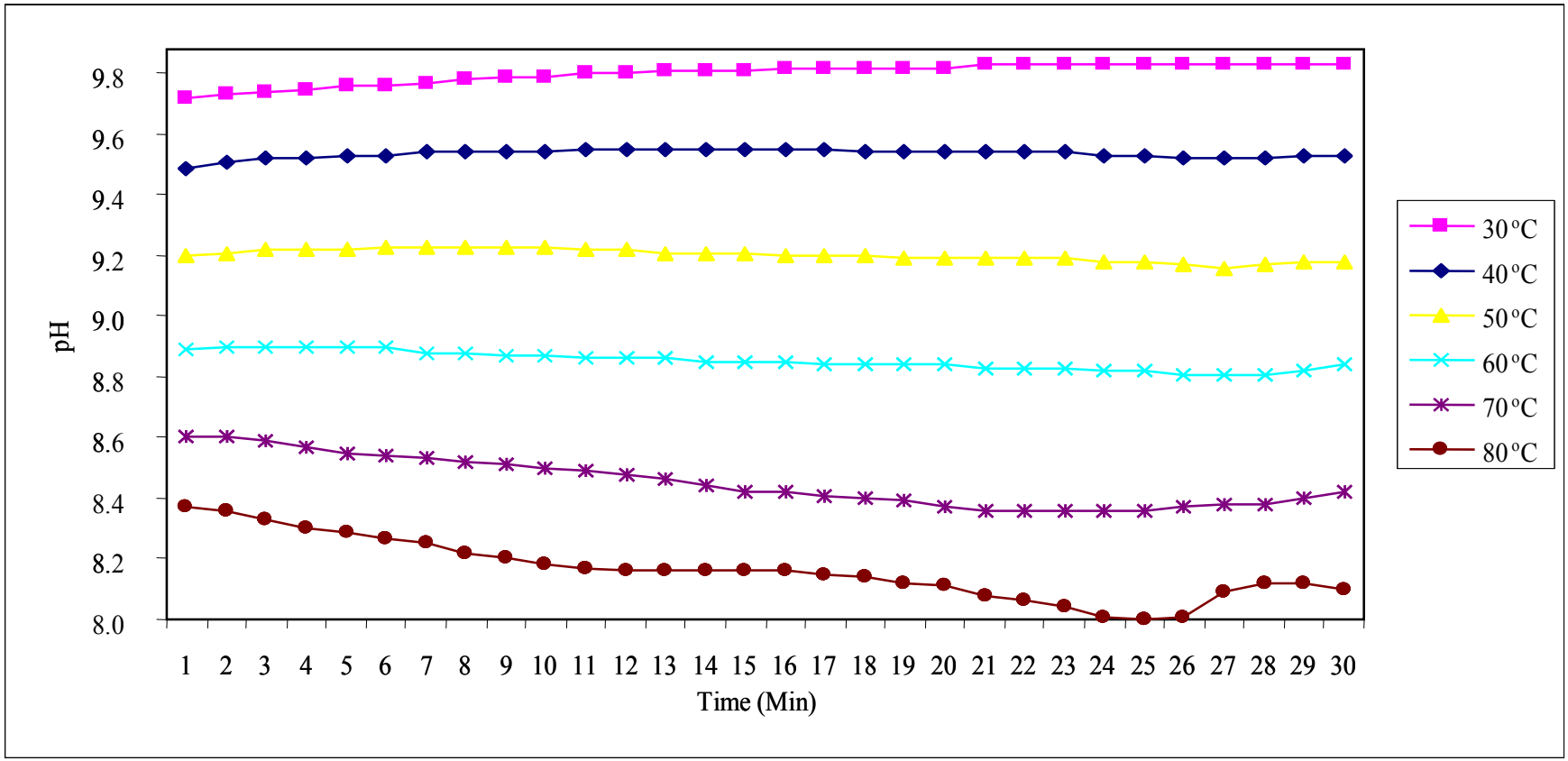

Figure B6. Variation of pH with temperature for the hydration of MgO in magnesium acetate

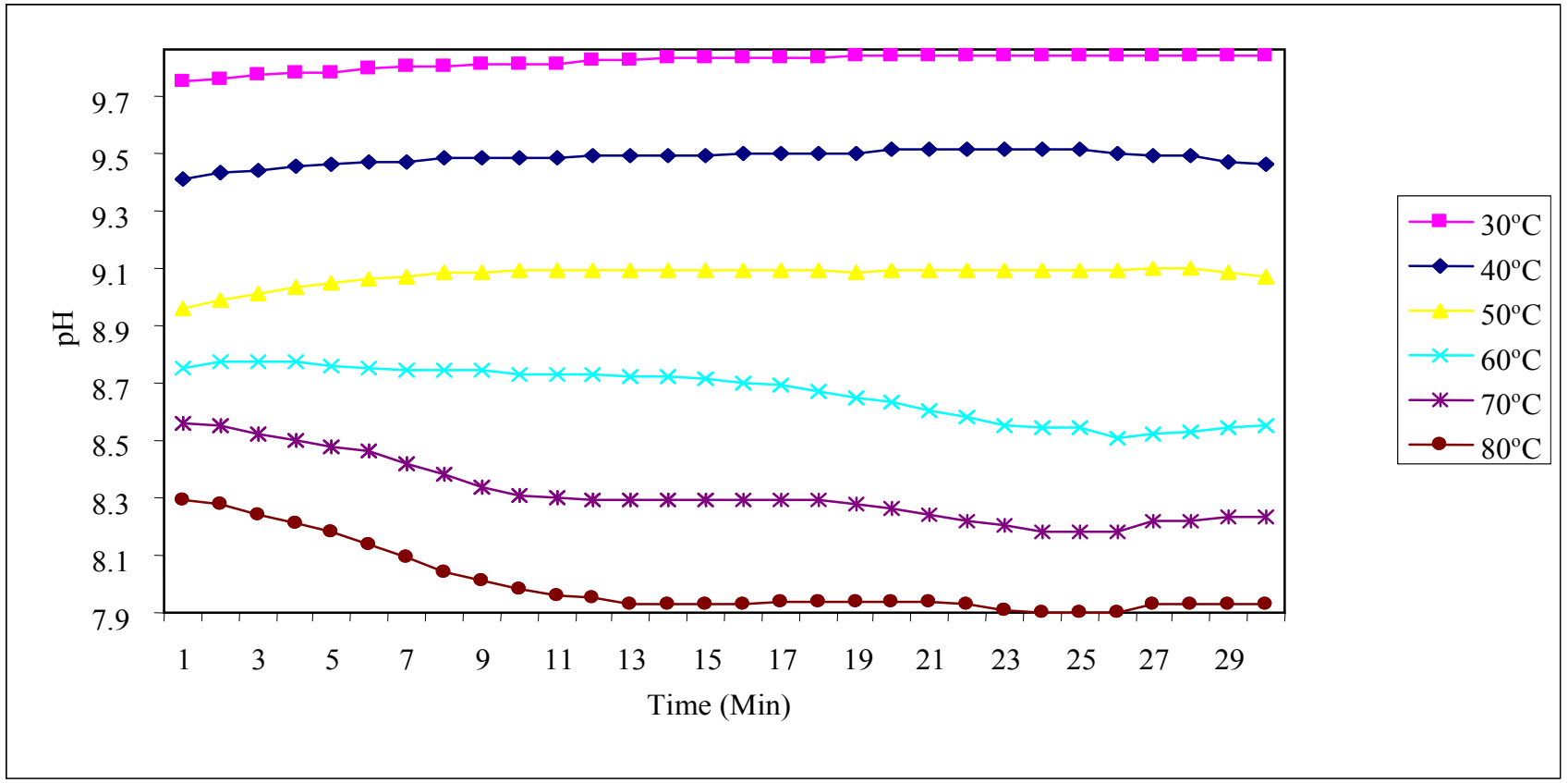

Figure B7. Variation of pH with temperature for the hydration of MgO in magnesium chloride

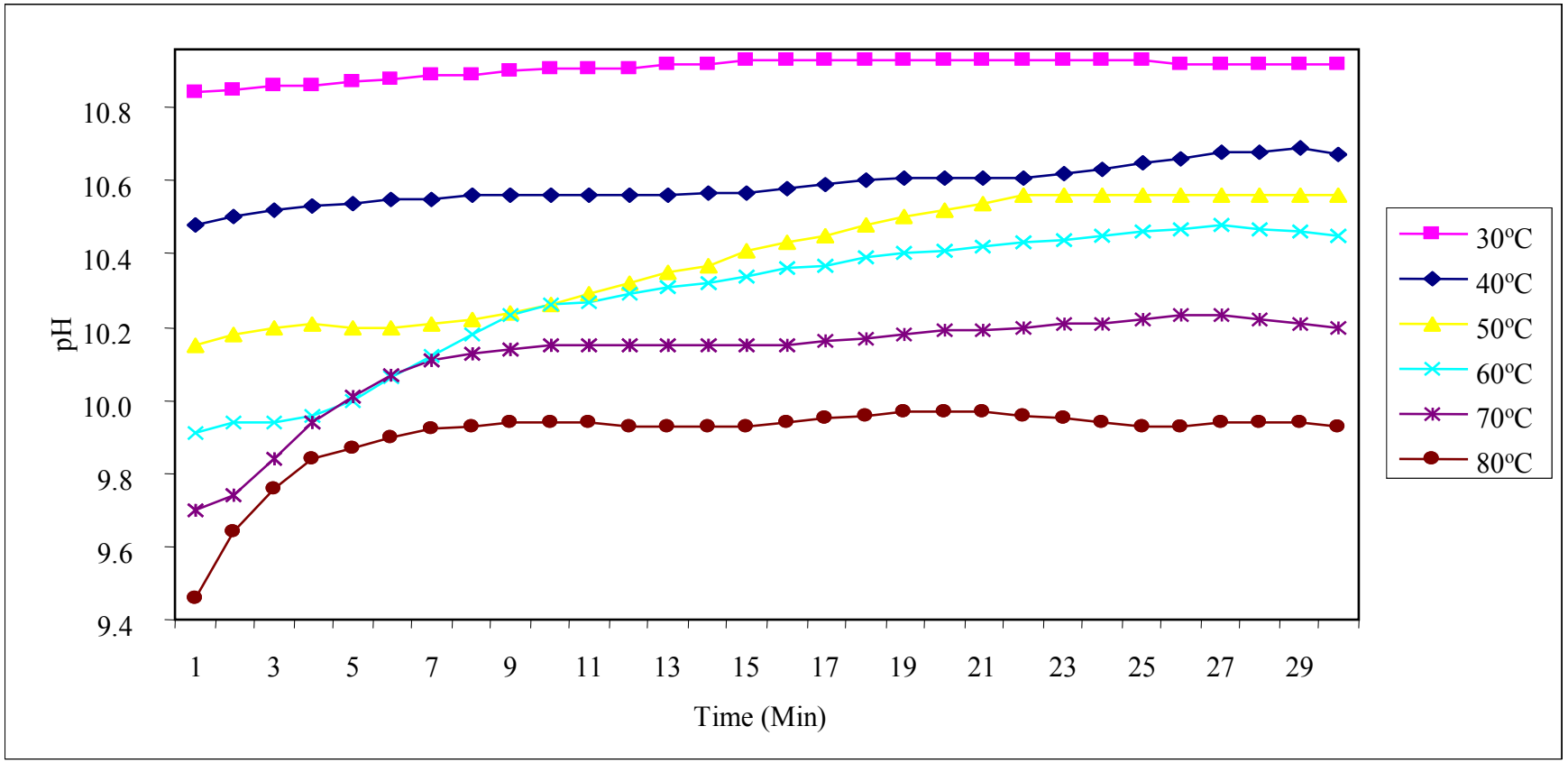

Figure B8. Variation of pH with temperature for the hydration of MgO in sodium acetate

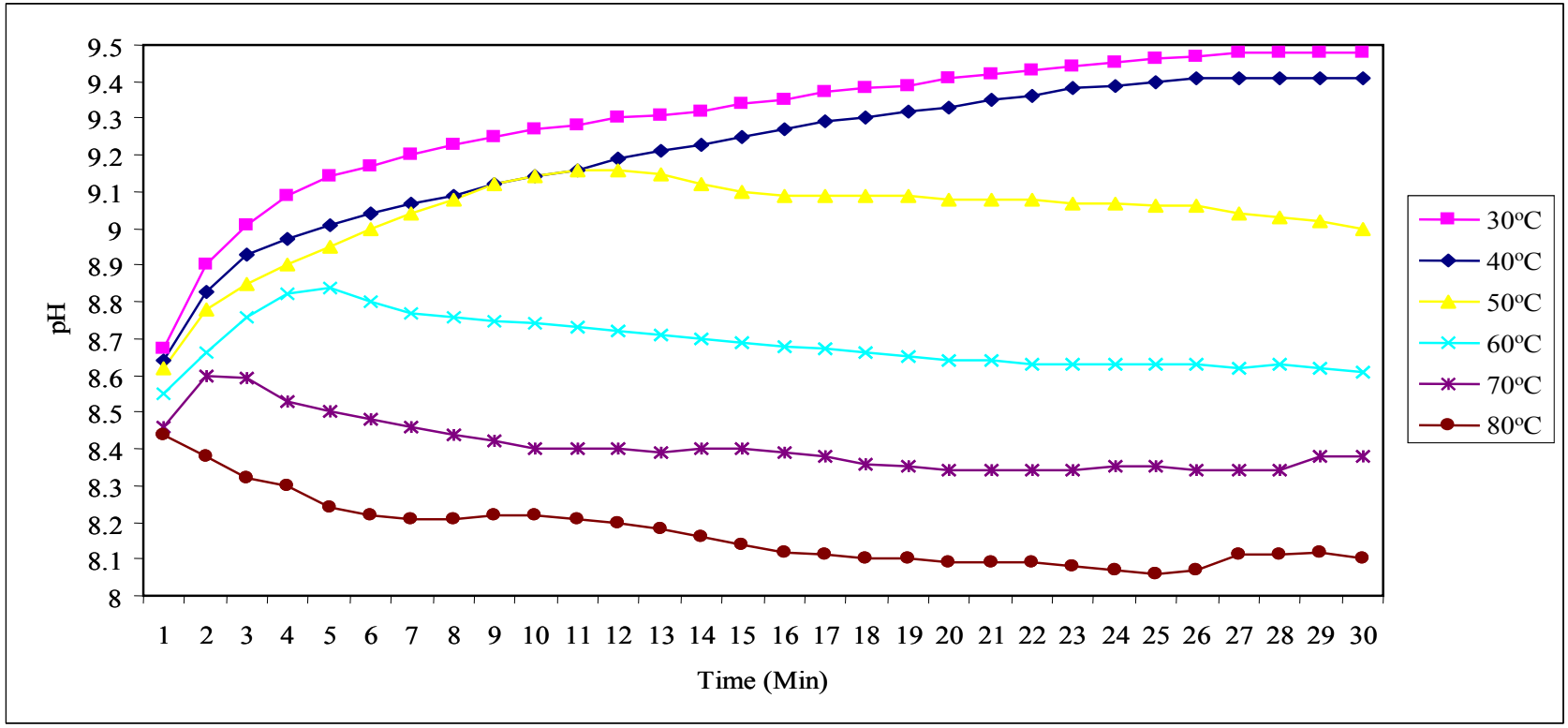

Figure B9. Variation of pH with temperature for the hydration of MgO in ammonium chloride

REFERENCES

ADAMSON, A.W., *Physical Chemistry of Surfaces*, John Wiley & Sons Inc., New York, 5th edition, (1990) 591-614.

AKIHIKO, H., European Patent, Appl., EP 599085 (1994), 11 pp.

ALVIN, R. and GUDOWSKI, R. PCT Int. Appl., WO 9424047 (1994), 18 pp.

ARAL, H., Hill, B. D. and SPARROW, G. J., *CSIR Minerals Report* DMR-2378C, 2004, p. 1-79.

BIRCHAL, V. S. S., ROCHA, S. D. F. and CIMINELLI, V. S. T., *Mineral Engineering*, **13 (14-15)** (2000) 1629-1633.

BIRCHAL, V. S., ROCHA, S. D. F., MANSUR, M. B. and CIMINELLI, V. S. T., *The Canadian Journal of Chemical Engineering*, **79** (2001) 507-511.

BOTHA, A. and STRYDOM, C. A., *Hydrometallurgy*, **62** (2001) 175.

BRATTON, R. J. and BRINDLEY, G. W., *Transactions of the Farady Society*, **61** (1965) 1017-1025.

BROWN, M. E., *Introduction to Thermal Analysis*, Chapman and Hall, New York, (1988) p. 7-21.

CANTERFORD, J. H., *Mineral Processing and Extractive Metallurgy Review*, (1985) 57-104.

DANIELS, T., *Thermal Analysis*, Kogan Page LTD, London, (1973) 38-58.

DE MILLE CAMPBELL, E., *Journal of Industrial and Engineering Chemistry*, **10** (1918) 595-6.

FILLIPOU, D., KATIFORIS, N., PAPASSIOPI, N. and ADAMS, K., *Journal of Chemical Technology and Biotechnology*, **74** (1999) 322-328

FILLIPOU, D., KATIFORIS, N., PAPASSIOPI, N. and ADAMS, K., *Journal of Chemical Technolology and Biotechnology*, **74** (2004) 322-338.

FIETKNECHT, W. and BRAUN, H., *Helvitica Chimica Acta*., **50 (7)** (1967) 2040.

FRUHWIRTH, O., HERZOG, G. W., HOLLER, L. and RACHETTI, A., *Surface Technology*, **21** (1985) 304-317.

GLASSON, D. R., *Journal of Applied Chemistry,* (London), **13** (1963) 119.

GREGG, S. J. and SING, K. S., *Adsorption Surface Area and Porosity*, Academic Press Inc., London, (1967) 35-73.

HAIR, M.L., Infrared Spectroscopy in Surface Chemistry, Marcel Dekker Inc., New York, (1967) 198-200.

HATAKEYAMA, T and LIU, Z., Handbook of Thermal Analysis, John Wiley and Sons, New York, (1998) 17-19.

HSU, JYH-PING. and NACU, A., *Colloids and Surfaces A: Physicochemical Engineering Aspects* **262** (2005) 220-231.

JOST, H., BRAUN, M. and CARIUS, CH., *Solid State Ionics*, **101-103** (1997) 221-228.

KIRK-OTHMER, *Encyclopedia of Chemical Technology*, 5th Edition, Vol. **15** (2005), p. 398-414.

LAYDEN, G. L. and BRINDLEY, G. W., *Journal of the American Ceramic Society*, **46 (11)** (1963) 518-522.

LOUBSER, M., *Introduction to X-ray Fluorescence Spectroscopy*, Course notes, University of Pretoria, (2005).

MARYSKA, M. and BLAHA, J., *Ceramics-Silikaty*, **41 (4)** (1997) 121-123.

MIKHAIL, R. S. and ROBENS, E., *Microstructure and Thermal Analysis of Solid Surfaces*, John Wiley & Sons, New York, (1983) 76-81.

MULLER, R. H. and MEHNERT, W., *Particle and Surface Characterisation Methods*, Medpharm Scientific Publishers Stuttgart, Germany, (1997) 189-195.

NAKAMURA, T. and NAKATANI, S., Japanese Patent, Kokai Tokkyo Koho, JP 0360774 (1989), 5 pp.

NAKANISHI, K., FUKUDA, T. and NOMURA, J., *Scientific Journal of the Ceramic Society of Japan*, **97** (1987) 683-689.

RASCHMAN, P. and FEDOROCKOVA, A., *Hydrometallurgy*, **71 (3-4)** (2004) 403-412.

ROCHA, S. D. F., MANSUR, M. B. and CIMINELLI, V. S. T., *Journal of Chemical Technolology and Biotechnology*, **79** (2004) 816-821.

SHINODA, H., Japanese Patent, Kokai Tokkyo Koho JP 0350665 (1989), 4 pp.

SMITH, K. A. and CRESSER, M. S., *Soil and Environmental Analysis, Modern Instrumental Technique*, 3rd Edition, Marcel Dekker Inc., New York, (2004) 283-290.

SMITHSON, G. L. and BAKHSHI, N. N., *TheCanadian Journal of Chemical Engineering*, **47** (1969) 508-513.

STRYDOM, C. A., VAN DER MERWE, E. M. and APHANE, M. E., *Journal of Thermal Analysis and Calorimetry*, **80** (2005) 659-662.

STUMM, W. and MORGAN, J. J., *Aquatic Chemistry*, Wiley Interscience, (1981) 583.

VAN DER MERWE, E. M., STRYDOM, C. A. and BOTHA, A., *Journal of Thermal Analysis and Calorimetry*, **77** (2004) 49-56.

VAN DER MERWE, E. M. and STRYDOM, C., *Journal of Thermal Analysis and Calorimetry,* **84 (2)** (2006) 467-471(5).

VERRYN, S., *Introduction to X-ray Powder Diffraction*, Course note, University of Pretoria, (2003).

WENDLANDT, W. W. M., *Thermal Methods of Analysis*, Interscience Publishers, New York, **19** (1964) 1-25.

WHITSON, C., *X-ray Methods*, John Wiley & Sons, London, (1987) 1-33.

WITKOWSKI, J. T., SMITH, D. M. and WAGER, M. T., PCT Int. App. (1996), 43.

Nova Operation Manual, Quantachrome Instruments (2002) 97-99.

URL-1 http://www.tateho.co.jp/e/develop/develop.html (Visited 21/06/2006).